Nuclotron-based
Ion Collider fAcility

Физика столкновений тяжелых ионов

В. Рябов

Heavy-ion collisions

- QCD is a fundamental theory of strong interactions
- Only colorless particles observed in the experiment (no free quarks or gluons) → confinement
- QGP is a state of matter in which quarks and gluons are free to move in space >> size of the nucleon
- QGP matter formation:

Two recipes:

(a) at high T - Early universe

(b) at high baryon density – Neutron stars

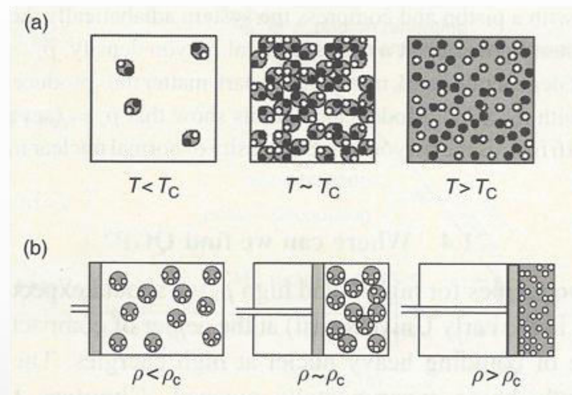

Relativistic heavy ion collisions - A combination of the two recipes

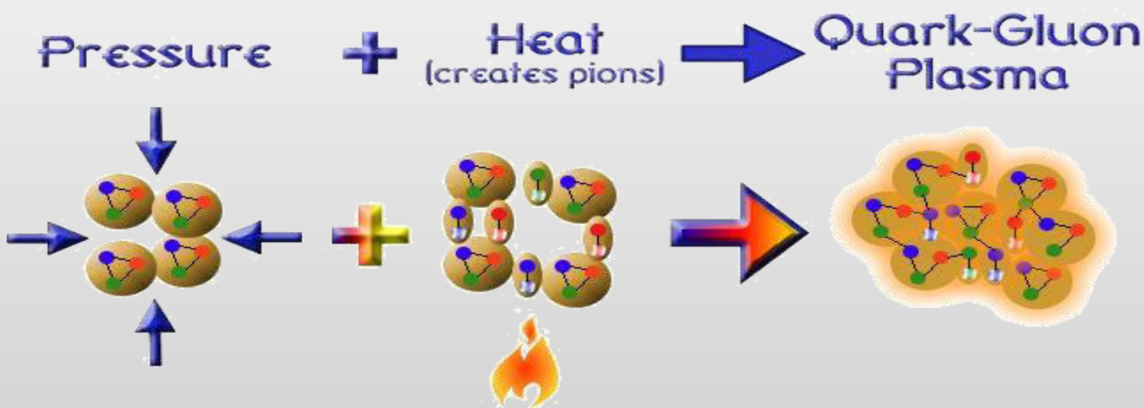

LQCD calculations

- The QGP is predicted by numerical calculations of QCD on the lattice

Bazavov et al., PLB 795,15 (2019)   PLB 478, 447 (2000)

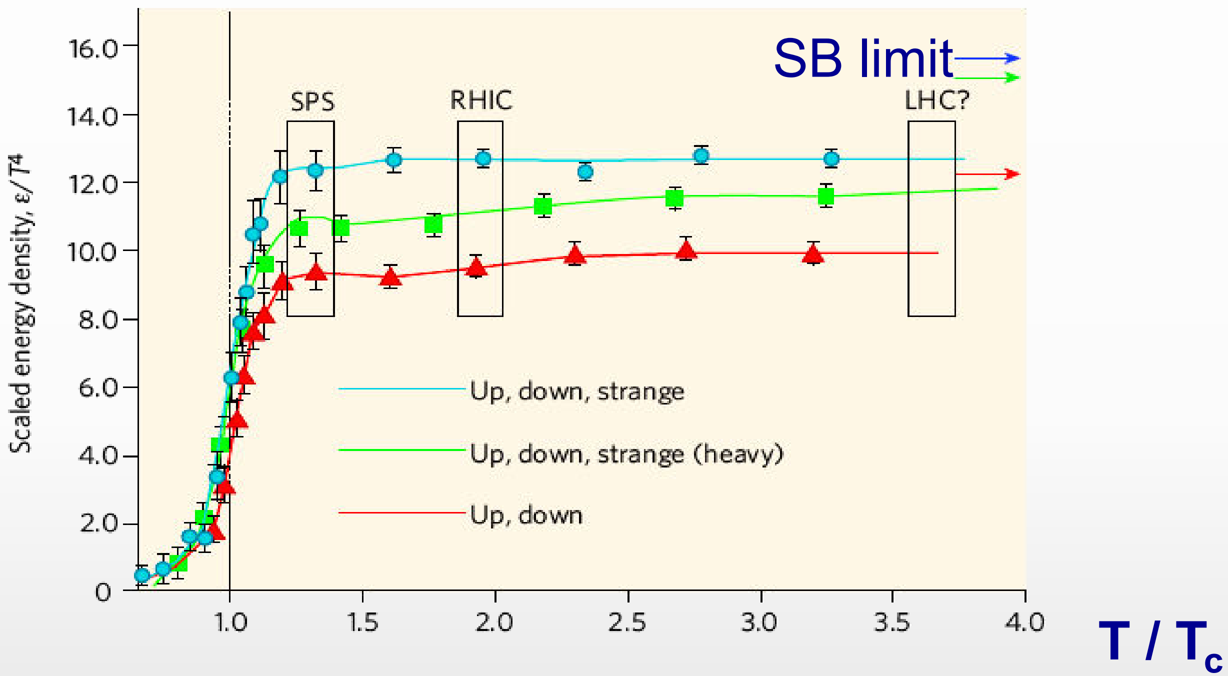

Recent LQCD calculations show that the critical temperature is: T_c (at $\mu_B = 0$) = 156.5 ± 1.5 MeV

- Accompanied by chiral symmetry restoration → constituent quark mass ~ 300 MeV turns into current quark mass ~ 5-10 MeV

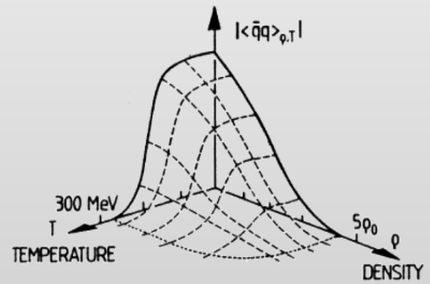

Heavy-ion collisions

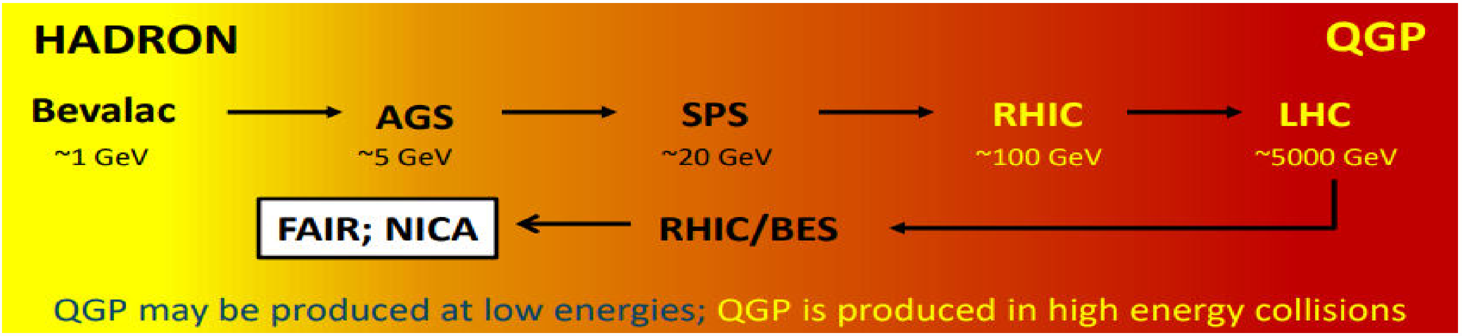

Short heavy-ion physics history

- **BEVALAC – LBNL** 1972-1984 max. $\sqrt{s_{NN}}$ = 2.2 GeV
- **SPS – CERN** 1986-2000 $\sqrt{s_{NN}}$ = 17.3 GeV — NA35/49, NA44, NA38/50/51, NA45, NA52, NA57, NA60, WA80/98, WA97 …
- **AGS – BNL** 1988-1996 $\sqrt{s_{NN}}$ = 4.8 GeV — E864/941, E802/859/866/917, E814/877, E858/878, E810/891, E896, E910 …
- **SIS18 – GSI** 1990 → $\sqrt{s_{NN}}$ = 2.4 GeV

(Fixed target)

- **RHIC – BNL** 2000-2025 $\sqrt{s_{NN}}$ = 200 GeV — BRAHMS, PHENIX, PHOBOS, STAR
- **LHC – CERN** 2010 → $\sqrt{s_{NN}}$ = 5.02 TeV — ALICE, ATLAS, CMS, LHCb

(Collider)

Near future

- NICA – JINR 2024 $\sqrt{s_{NN}}$ = 11 GeV — MPD, BM@N — Collider & Fixed target
- SIS100 – FAIR 2028? $\sqrt{s_{NN}}$ = 5 GeV — CBM, HADES — Fixed target

Heavy-ion collisions

- Study QCD under extreme conditions of temperature and density
- Explore the QCD phase diagram, search for the QGP and study its properties

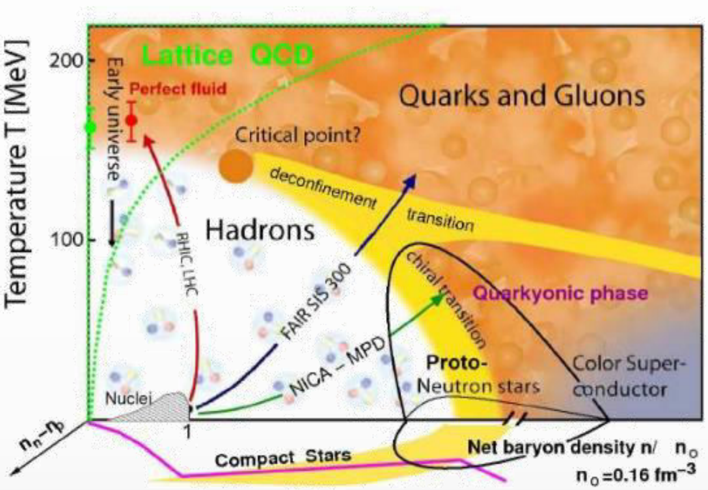

Why Quark-gluon plasma is of interest?

- ✓ primordial form of QCD matter at high temperatures and/or (net)baryon densities
- ✓ present during the first microseconds after Big Bang and in cores of the compact neutron stars / mergers
- ✓ provides important insights on the origin of mass for matter, and how quarks are confined into hadrons

<u>High beam energies ($\sqrt{s_{NN}}$ > 100 GeV)</u>

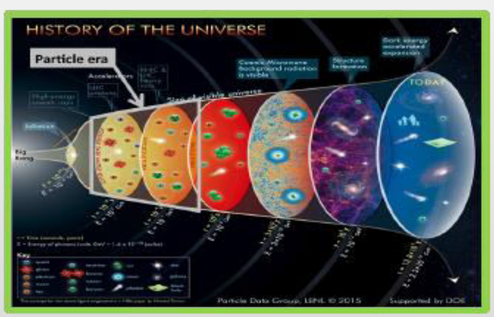

High temperature:
Early Universe evolution

<u>Low beam energies ($\sqrt{s_{NN}}$~ 10 GeV)</u>

High baryon density:
Inner structure of
compact stars

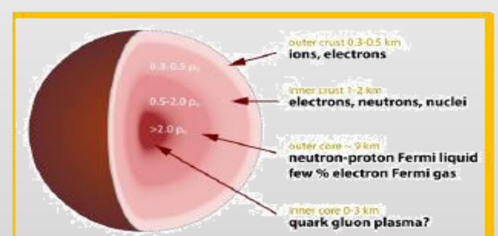

System evolution in heavy-ion collisions

Fireball is ~10^{-15} meters across and lives for 5×10^{-23} seconds

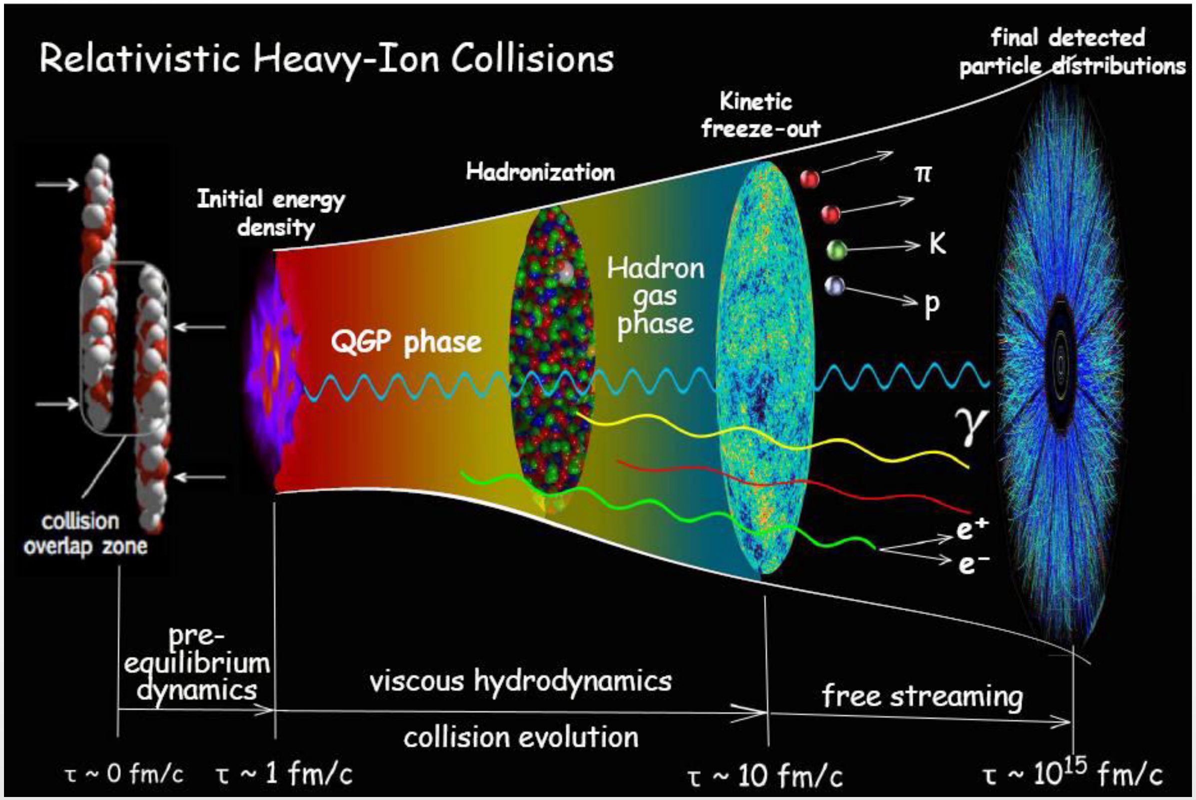

- Only final state particles are measured in the detector: γ, $e^{\pm}$, $\mu^{\pm}$, π^0, $\pi^{\pm}$, K^0, $K^{\pm}$, η, ω, p, $\bar{p}$, ϕ, Λ, Σ, Ξ, etc.
- The measurements are used to infer properties of the early state of relativistic heavy-ion collisions by comparing measurement results with model (post)predictions

Initial state

QGP as a relativistic fluid

Collective flow

Anisotropic flow at RHIC/LHC

❖ Initial eccentricity and its fluctuations drive momentum anisotropy v_n with specific viscous modulation

Spatial anisotropy of the nuclear overlap region

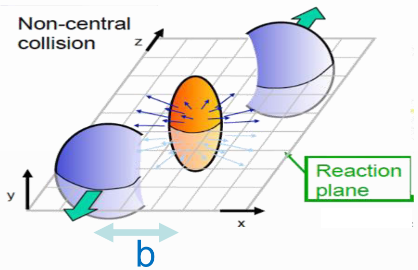

$$\epsilon_n = \sqrt{\frac{\langle r^n \cos n\phi\rangle + \langle r^n \sin n\phi\rangle}{\langle r^n\rangle}}$$

$\epsilon_n \propto v_n$

Azimuthal distribution of produced particles wrt to reaction plane (Ψ_n)

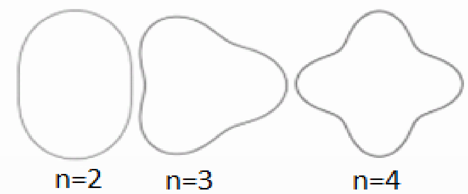

$$\frac{dN}{d\phi} \propto \left(1 + 2\sum_{n=1} v_n \cos\left[n\left(\phi - \Psi_n\right)\right]\right)$$

Anisotropic flow: $v_n = \langle\cos[n(\varphi - \Psi_n)]\rangle$

❖ Evidence for a dense perfect liquid found at RHIC/LHC (M. Roirdan et al., Scientific American, 2006)

Gale, Jeon et al., Phys. Rev. Lett. 110, 012302

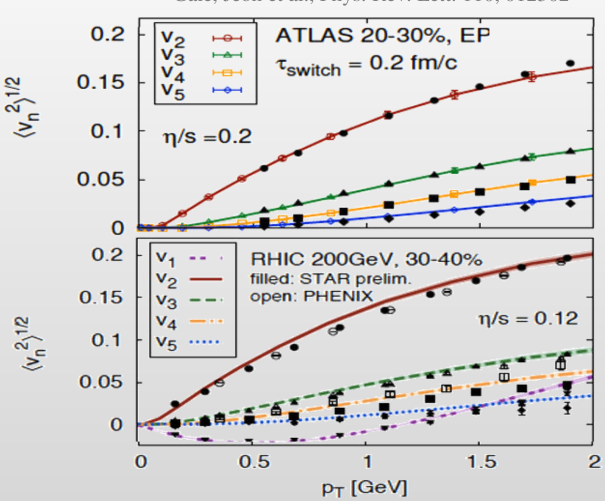

Phys.Rev.C 92 (2015) 3, 034913

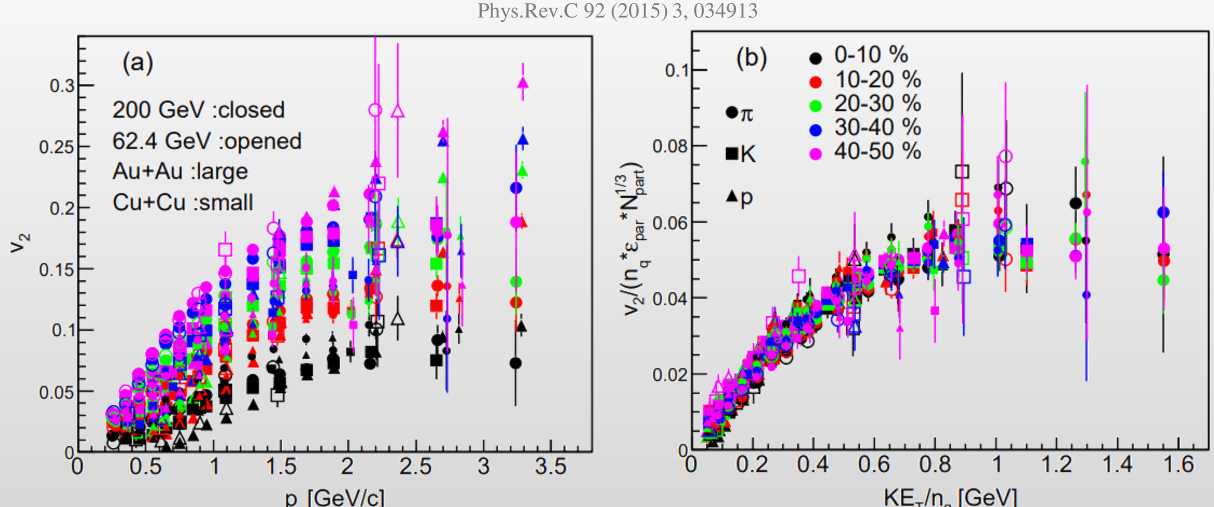

❖ System size scan (A-A): initial geometry → flow harmonics → $\frac{\eta}{s}(T,\mu), \frac{\zeta}{s}(T,\mu), c_s(T), \alpha_s(T), etc.$

Small system scan at RHIC

- v_2 and v_3 measurements in p-Au, d-Au and ^{3}He-Au @ 200 GeV by PHENIX

Nature Phys. 15 (2019) 3, 214-220

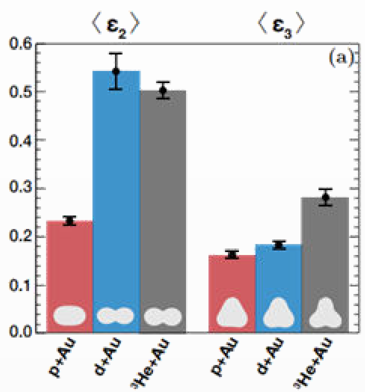

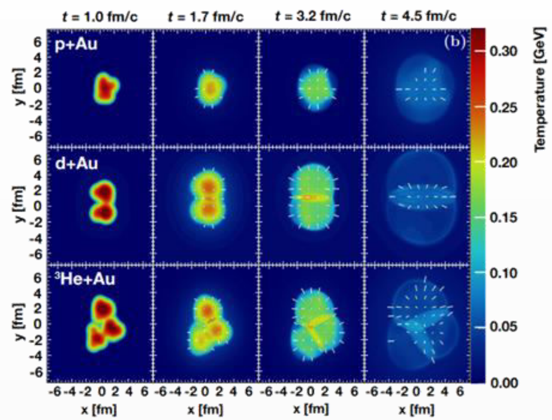

- Measurements demonstrate that the v_n's are correlated to the initial geometry
- Hydrodynamic models, which include the formation of short-lived QGP droplets, provide a simultaneous description of these measurements

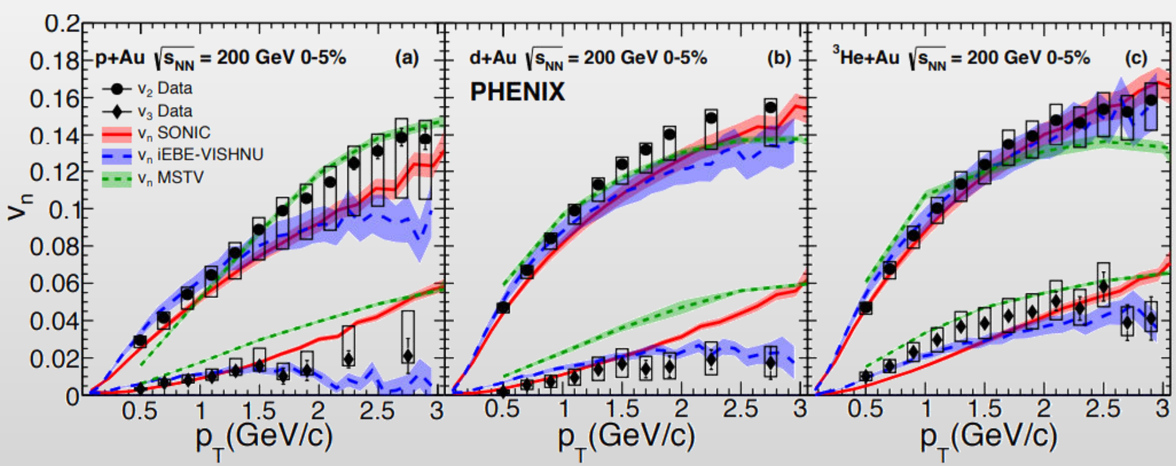

Beam energy dependence

- At lower energies, flow is highly sensitive to fireball expansion and interactions with spectators
  - ✓ RHIC @ 200 GeV (2R/γ) ~ 0.1 fm/c
  - ✓ AGS @ 3-4.5 GeV (2R/γ) ~ 9-5 fm/c
- Sensitivity to EOS, v_1 and v_2 show strong centrality, energy and species dependence
- Flow probes dominant degrees of freedom (hadronic vs. partonic)

Phys.Rev.Lett. 112 (2014) 16, 162301

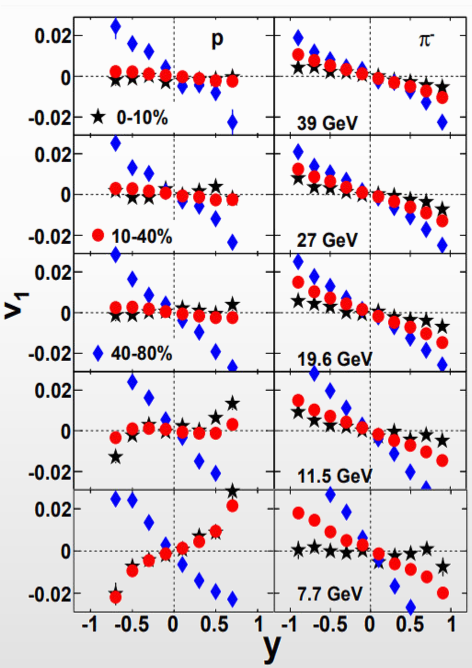

✓ models do not quite reproduce the measurements

EPJ Web Conf. 204 (2019) 03009

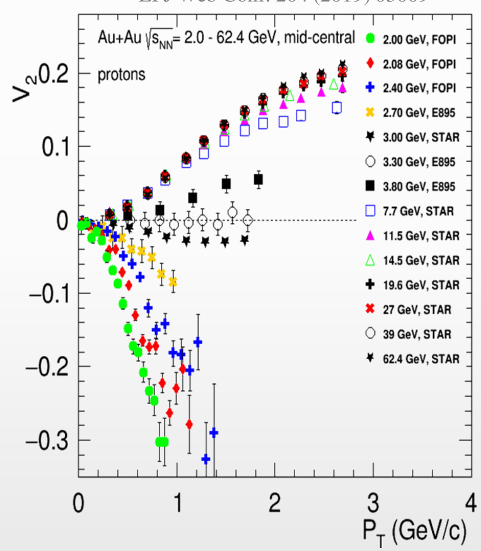

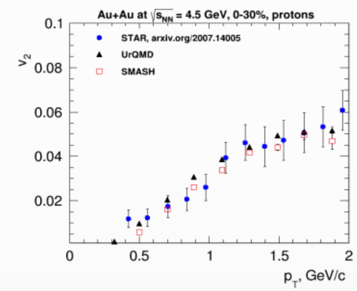

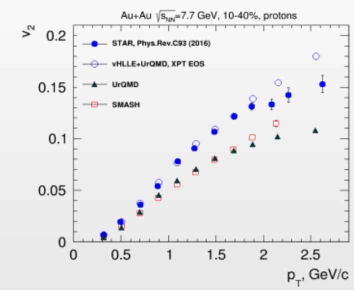

✓ $\sqrt{s_{NN}}$ ~ 3-4.5 GeV, pure hadronic models reproduce v_2 (JAM, UrQMD) → degrees of freedom are the interacting baryons

✓ $\sqrt{s_{NN}} \geq 7.7$ GeV, need hybrid models with QGP phase (vHLLE+UrQMD, AMPT with string melting,…)

NICA: <u>system size scan</u> for flow measurements to better understand the medium transport properties and onset of the phase transition → <u>unique capability at NICA</u>

Global polarization of particles

Non-central heavy-ion collisions

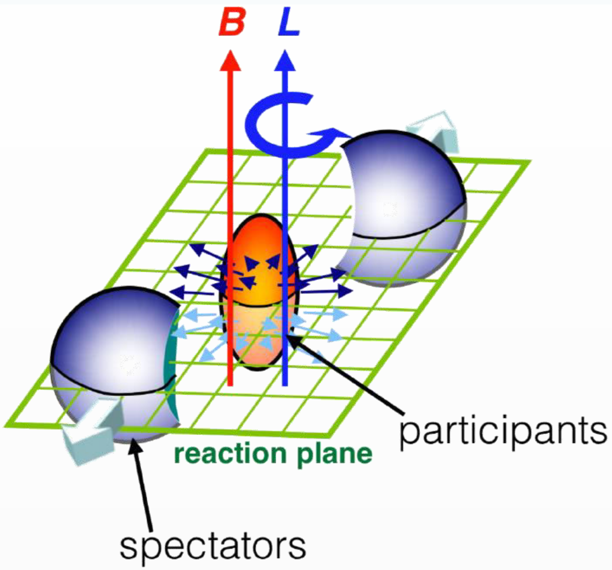

Large angular momentum due to medium rotations

Beccattini et al., PRC 77 (2008) 024906

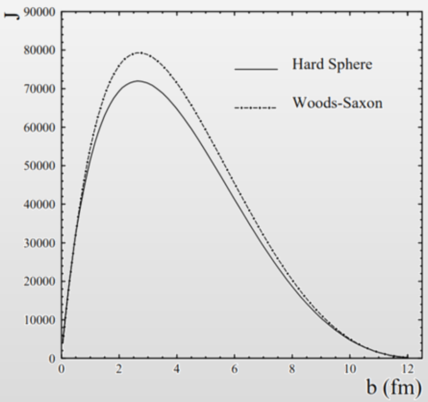

Strong magnetic field (~ 10^{13} T) formed for a short period of time

Kharzeev et al., NPA 803 (2008)

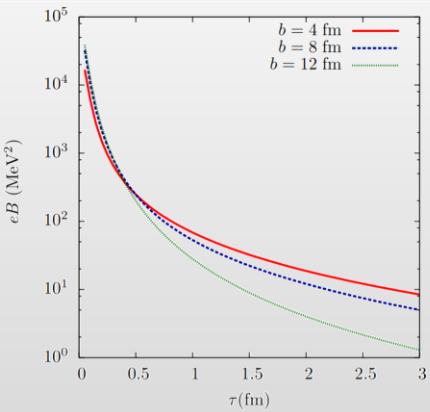

Focus is to see the effect of large angular momentum and magnetic field in heavy-ion collisions

Global hyperon polarization

- Large angular momentum and strong magnetic field formed in mid-central heavy-ion collisions → polarization of particles in the final state

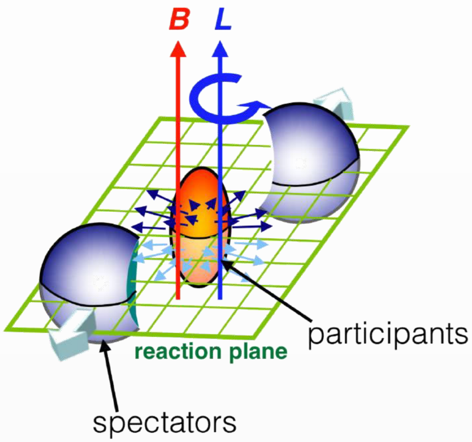

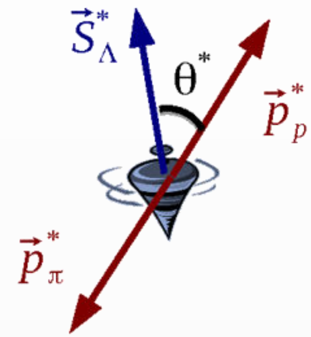

- $\Lambda/\bar{\Lambda}$ are "self-analyzing" probes → preferential emission of proton in spin direction

STAR, Nature 548, 62 (2017)

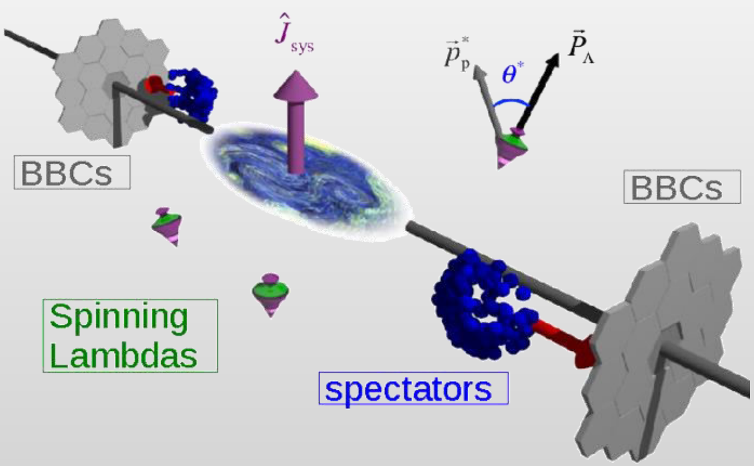

Phys.Rev.Lett.94:102301,2005;
Erratum-ibid.Lett.96:039901,2006

The global polarization observable is defined by [34]:

$$P_\Lambda = \frac{8}{\pi\alpha_\Lambda}\frac{\langle \sin(\Psi_{EP} - \phi^*_p)\rangle}{R_{EP}}. \quad (1)$$

Here $\alpha_\Lambda = 0.732 \pm 0.014$ [35] is the Λ decay parameter, Ψ_{EP} the event plane angle, ϕ^*_p the azimuthal angle of the proton in the Λ rest frame, R_{EP} the resolution of the event plane angle and the brackets $\langle . \rangle$ denote the average

Global hyperon polarization

- ❖ Global hyperon polarization measurements in mid-central A+A collisions at $\sqrt{s_{NN}}$= 3-5000 GeV

STAR, Phys.Rev.C, 104(6):L061901, 2021

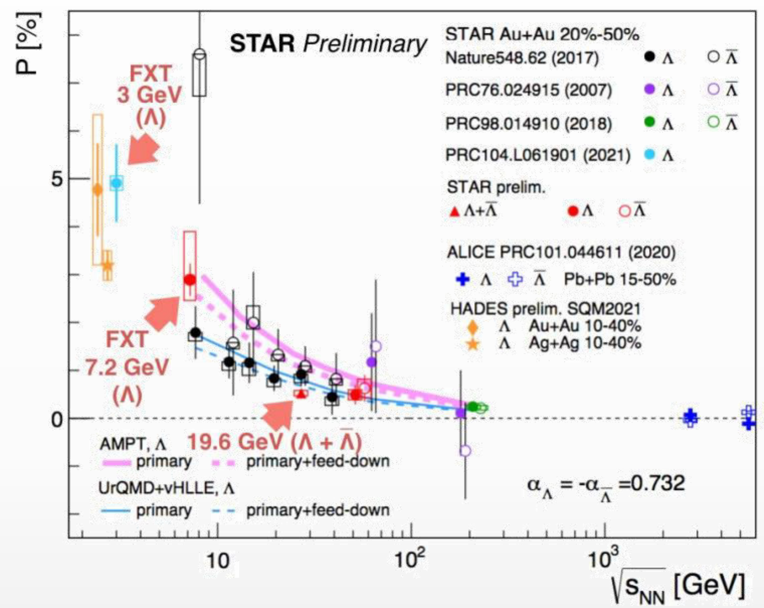

- ❖ Global polarization of hyperons experimentally observed, decreases with $\sqrt{s_{NN}}$
- ❖ Hint for a Λ-$\overline{\Lambda}$ difference, magnetic field, $P_\Lambda \simeq \frac{1}{2}\frac{\omega}{T} + \frac{\mu_\Lambda B}{T}$, $P_{\bar{\Lambda}} \simeq \frac{1}{2}\frac{\omega}{T} - \frac{\mu_\Lambda B}{T}$?
- ❖ Energy dependence of global polarization is reproduced by AMPT, 3FD, UrQMD+vHLLE
- ❖ AMPT with partonic transport strongly underestimates measurements at $\sqrt{s_{NN}}$ = 3 GeV → hadron gas?

NICA: contribute <u>extra points in the energy range 2-11 GeV</u> with small uncertainties;
centrality, p_T and rapidity dependence of polarization not only for Λ, but other (anti)hyperons (Λ, Σ, Ξ)

Polarization of vector mesons: $K^*(892)$ and ϕ

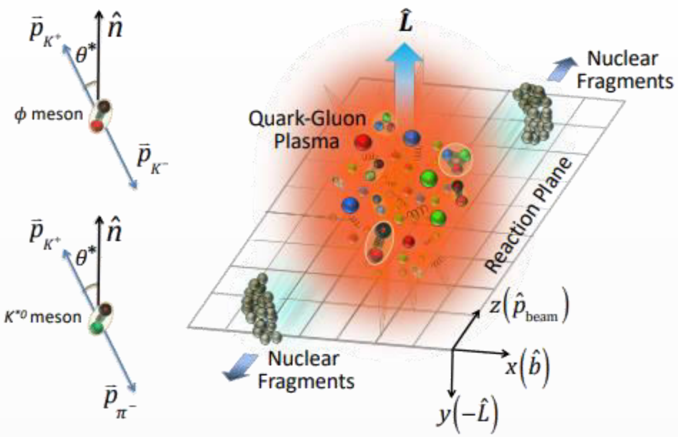

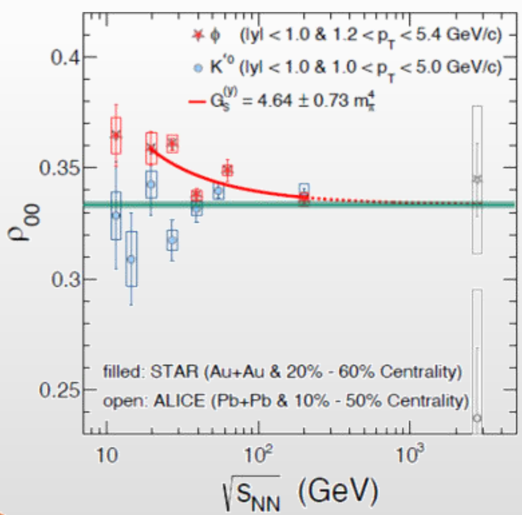

- Light quarks can be polarized by $|\bar{J}|$and $|\bar{B}|$
- If vector mesons are produced via recombination their spin may align
- Quantization axis:
  - ✓ normal to the production plane (momentum of the vector meson and the beam axis)
  - ✓ normal to the event plane (impact parameter and beam axis)
  - ✓ ρ_{00} (PP) - $\frac{1}{3}$ =[ρ_{00} (EP) - $\frac{1}{3}$] [$\frac{1+3v_2}{4}$]
- Measured as anisotropies:

$$\frac{dN}{dcos\theta} = N_0\left[1 - \rho_{0,0} + cos^2\theta\left(3\rho_{0,0} - 1\right)\right]$$

$\rho_{0,0}$ is a probability for vector meson to be in spin state = 0
→ $\rho_{0,0}$ = 1/3 corresponds to no spin alignment

- Measurements at RHIC/LHC challenge theoretical understanding → ρ_{00} can depend on multiple physics mechanisms (vorticity, magnetic field, hadronization scenarios, lifetimes and masses of the particles)

NICA: <u>extend measurements</u> in the NICA energy range, $\sqrt{s_{NN}}$ < 11 GeV

Initial state

QGP as a relativistic fluid

Strangeness production

Strangeness production: pp, p-A, A-A

- Since the mid 80s, strangeness enhancement is considered as a signature of the QGP formation
- Experimentally observed in heavy-ion collisions at AGS, SPS, RHIC and LHC energies

NA57 and WA97 at SPS

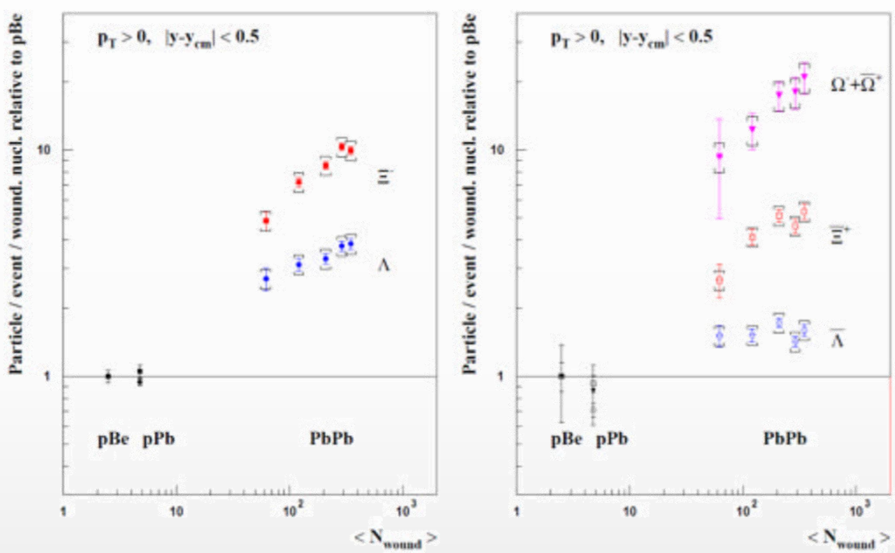

ALICE @ LHC

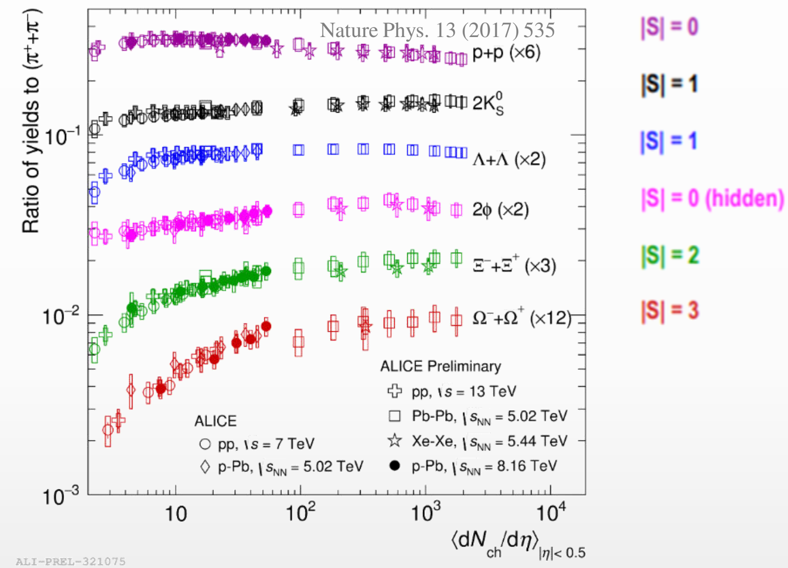

- Smooth evolution vs. multiplicity in pp, p-A and A-A collisions at LHC energies
- Strangeness enhancement increases with strangeness content and particle multiplicity
- STAR @ RHIC measurements in pp, A-A are in agreement with ALICE @ LHC at similar $\langle dN_{ch}/d\eta \rangle$
- Stronger relative enhancement at lower collision energies

Origin of enhancement

- ❖ No consensus on the dominant strangeness enhancement mechanisms:
  - ✓ strangeness enhancement in QGP contradicts with the observed collision energy dependence
  - ✓ strangeness suppression in pp within canonical suppression models reproduces most of results except for ϕ(1020)

Nature Physics volume 13, pages535–539 (2017)

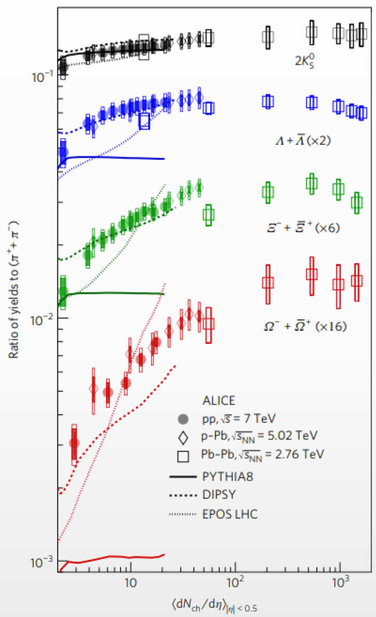

V. Vislavicius, A. Kalweit, arXiv:1610.03001

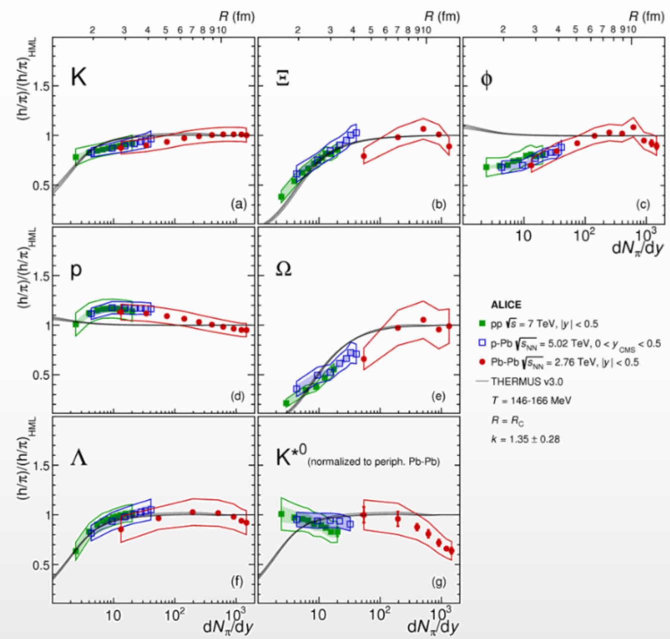

- ❖ System size scan for (multi)strange baryon and meson production in p+p, p+A and A+A collisions is a key to understanding of strangeness production:
  - ✓ excitation function of hadrons (yields, spectra, and ratios)
  - ✓ probe early stage and phase transformations in QCD medium, nuclear matter EOS and chemical equilibration

System size scan is <u>unique capability</u> of NICA in the energy range

Light (hyper)nuclei

- Production mechanism usually described with two classes of phenomenological models :
  - ✓ statistical hadronization (SHM) → production during phase transition, $dN/dy \propto \exp(-m/T_{chem})$
  - ✓ coalescence → (anti)nucleons close in phase space ($\Delta p < p_0$) and matching the spin state form a nucleus
- Hypernuclei measurement studies are crucial:
  - ✓ microscopic production mechanism, Y-N (Y-Y, Y-N-N) potentials, strange sector of nuclear EoS
  - ✓ strong implications for astronuclear physics → hyperons expected to exist in the inner core of neutron stars
- Models predict enhanced hypernuclei production at NICA→ double hypernuclei are reachable

A. Andronic et al, PLB 697 (2011) 203

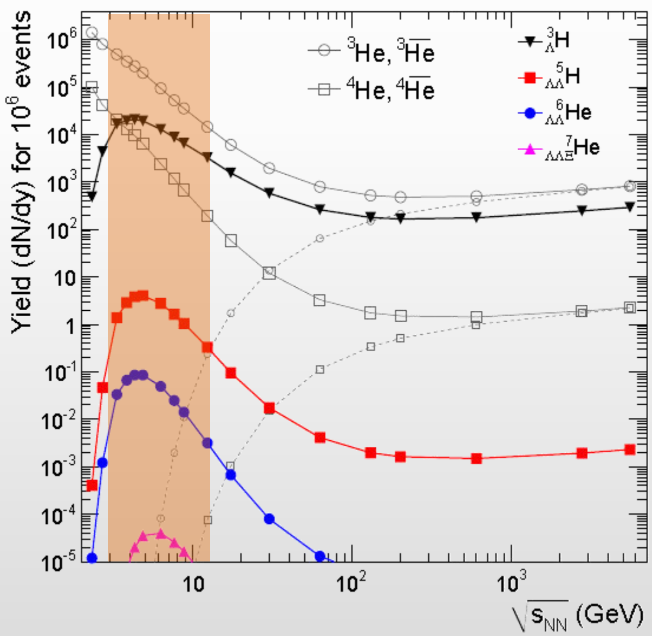

QM’2022

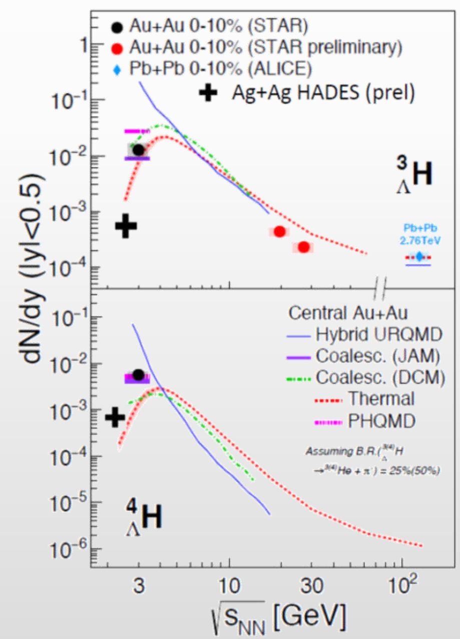

Yields, lifetimes and binding energies are needed at NICA energies to provide tighter constrains

Hadronic resonances

Hadronic phase

- A phase between chemical and kinetic freeze out → lifetime and conditions?
- Short-lived resonances are sensitive to rescattering and regeneration in the hadronic phase

	ρ(770)	K^*(892)	Σ(1385)	Λ(1520)	Ξ(1530)	ϕ(1020)
cτ (fm/c)	1.3	4.2	5.5	12.7	21.7	46.2
$\sigma_{rescatt}$	$\sigma_\pi\sigma_\pi$	$\sigma_\pi\sigma_K$	$\sigma_\pi\sigma_\Lambda$	$\sigma_K\sigma_p$	$\sigma_\pi\sigma_\Xi$	$\sigma_K\sigma_K$

- Reconstructed resonance yields in heavy ion collisions are defined by:
  - ✓ resonance yields at chemical freeze-out
  - ✓ hadronic processes between chemical and kinetic freeze-outs:

    rescattering: daughter particles undergo elastic scattering or pseudo-elastic scattering through a different resonance → parent particle is not reconstructed → loss of signal

    regeneration: pseudo-elastic scattering of decay products ($\pi K \to K^{*0}$, $KK \to \phi$ etc.) → increased yields

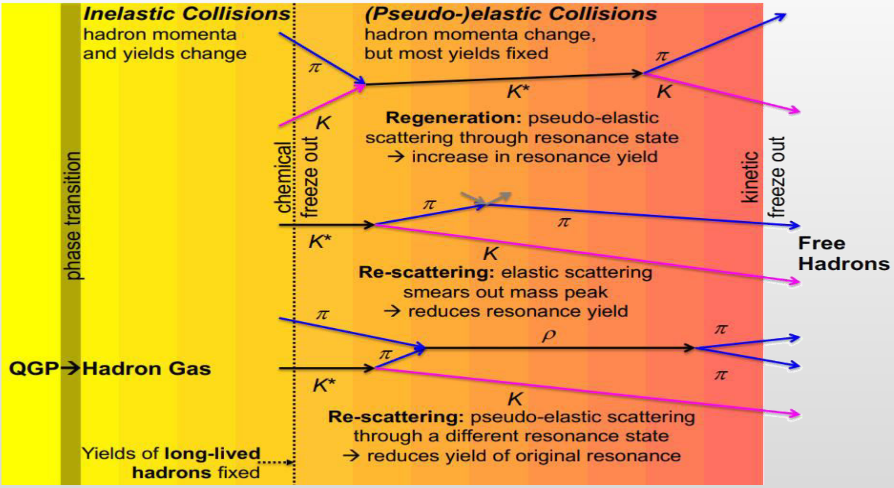

- Resonances provide the means to directly probe the hadronic phase properties

Experimental results

- Properties of the hadronic phase are studied by measuring ratios of resonance yields to yields of long-lived particles with same/similar quark contents: ρ/π, K^*/K, ϕ/K, Λ^*/Λ, $\Sigma^{*\pm}/\Sigma$ and Ξ^{*0}/Ξ

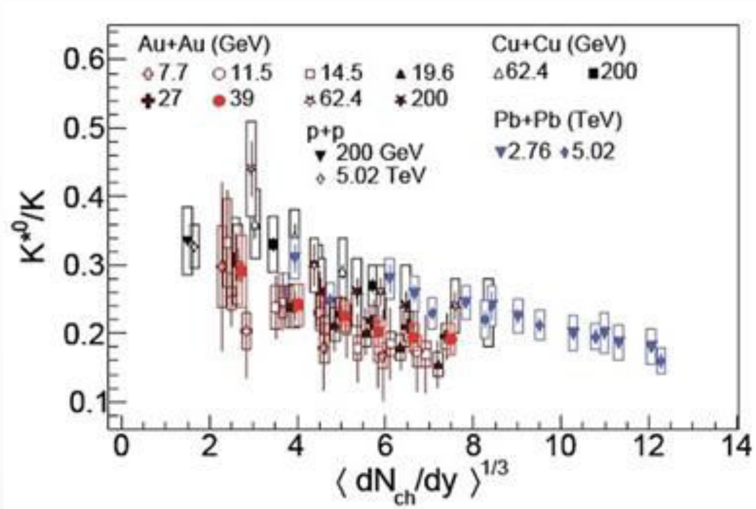

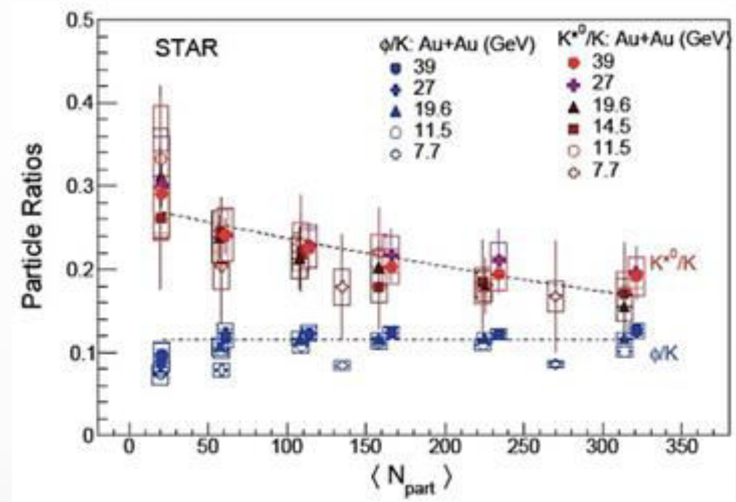

- ✓ suppressed production of short-lived resonances (τ < 20 fm/c) in central A+A collisions → rescattering takes over the regeneration
- ✓ no modification for longer-lived resonances, ϕ-meson (τ ~ 40 fm/c)
- ✓ yield modifications depend on event multiplicity, not on collision system/energy

- Measurements in a wide energy range $\sqrt{s_{NN}}$= 7-5000 GeV support the existence of a hadronic phase that lives long enough (up to τ ~ 10 fm/c) to cause a significant reduction of the reconstructed yields of short-lived resonances
- All model predictions must be filtered through the hadronic phase

Precise measurements at NICA are needed to validate description of the hadronic phase in models

Initial state

QGP as a relativistic fluid

Electromagnetic radiation

Direct photons and system temperature

- Direct photons are all photons except for those coming from hadron decays:
  - ✓ produced during all stages of the collision
  - ✓ QGP is transparent for photons → penetrating probe

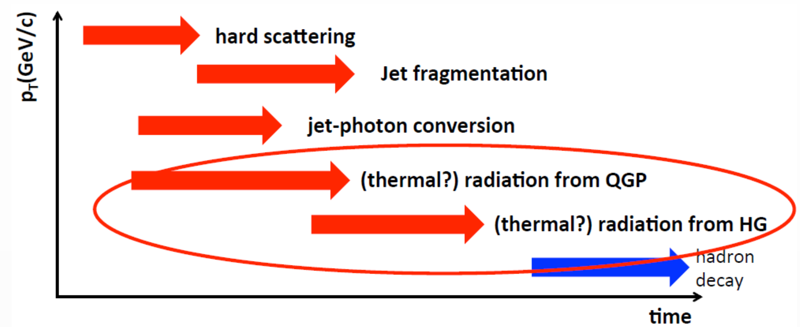

- Low-E photons → effective temperature of the system:

$$E_\gamma \frac{d^3 N_\gamma}{d^3 p_\gamma} \propto e^{-E_\gamma / T_{\mathrm{eff}}}$$

- Relativistic A+A collisions → the highest temperature created in laboratory ~ 10^{12} K

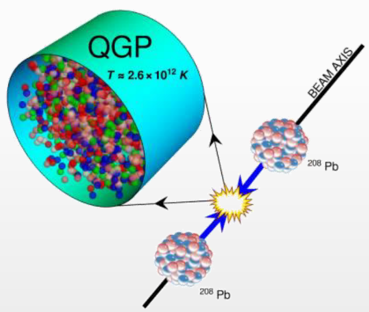

Temperature at the center of the Sun ~ 15 000 000 K

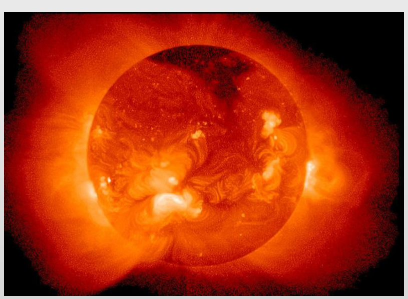

A medium of ~ 200 MeV is 100 000 times hotter !!!

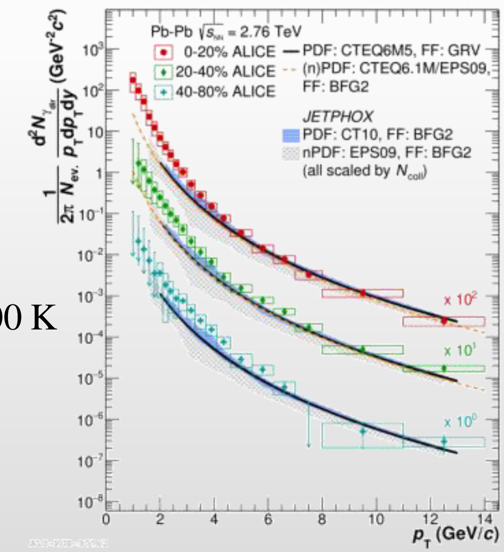

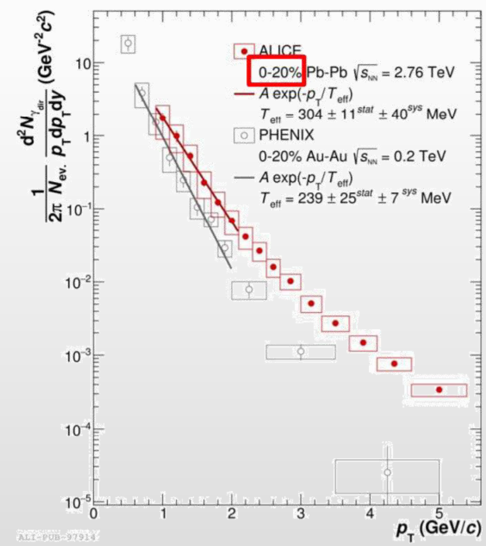

T_{eff} ~ 240 MeV at RHIC; T_{eff} ~ 300 MeV at the LHC

T_{eff} >> T_c ~ 150 MeV predicted by LQCD

Direct photons puzzle(s)

- Simultaneous description of direct photon yields and elliptic flow (v_2) is problematic:
  - ✓ direct photon flow is similar to flow of decay photons, underestimated by hydro → favors late emission
  - ✓ large yields of low-E direct photon yields require early emission in to be described by hydro models

PRC 79 (2009) 021901

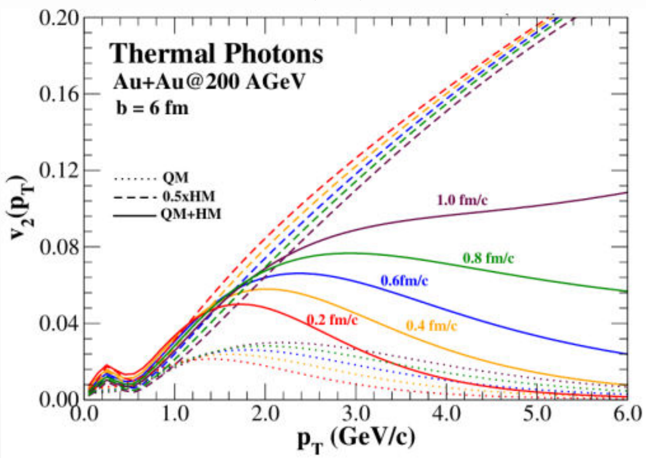

Phys.Lett.B 789 (2019) 308-322

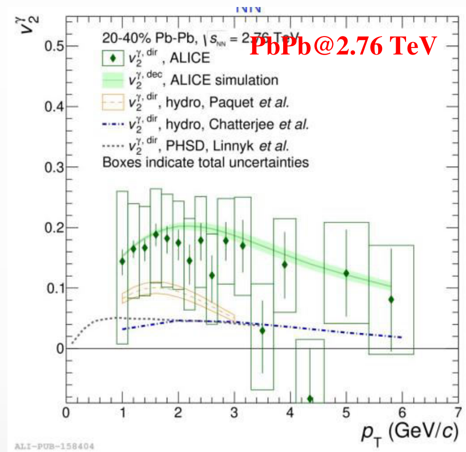

Phys.Rev. C94 (2016) no.6, 064901

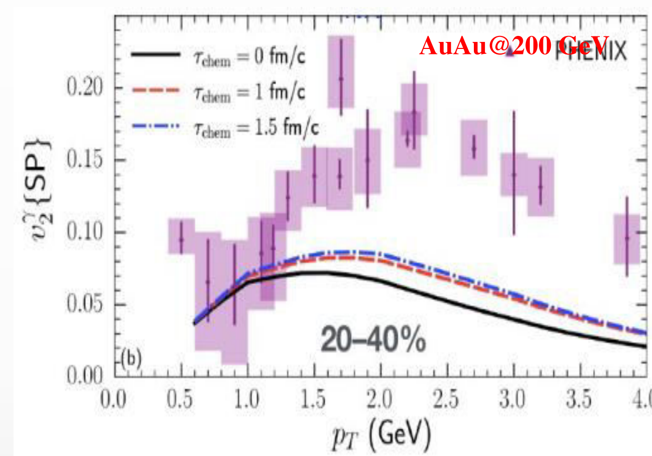

- Controversial results reported for different systems by different experiments

Quark Matter 2019, arxiv 2002.05191

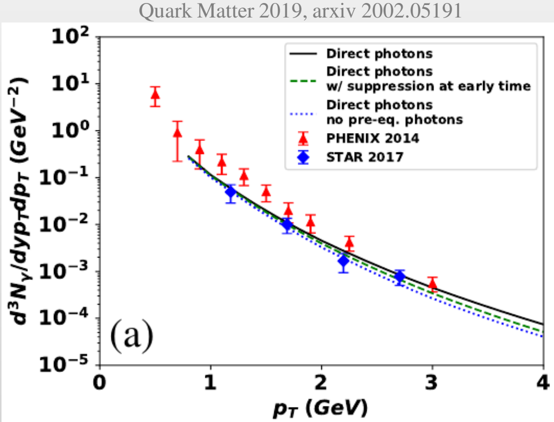

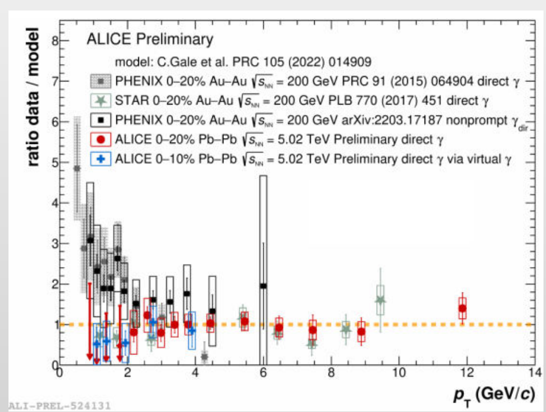

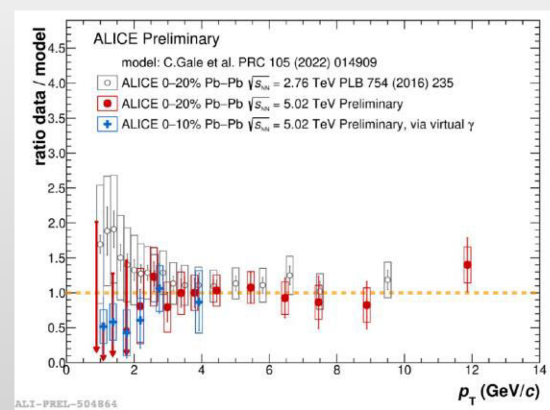

Expectations for NICA

- Experimental measurements in A+A collisions are available from the LHC (2.76-5 TeV), RHIC (62-200 GeV) and WA98 (17.2 GeV)
- No measurements at NICA energies (direct photon yields and flow vs. p_T and centrality)

Estimation of the direct photon yields @NICA

model calculations

empirical scaling

- o UrQMD v3.4 with hybrid model (3+1D hydro, bag model EoS, hadronic rescattering and resonances within UrQMD)
- o Each cell have Ti, Ei, μbi:
  - T is high – QGP phase (Peter Arnold, Guy D. Moore, Laurence G. Yaffe, JHEP 0112:009 2001)
  - T is low – HG phase (Simon Turbide, Ralf Rapp, Charles Gale, Phys.Rev.C69:014903,2004)
  - T is intermediate – mixed phase
- o Integrate over all cells and all time steps
- o Calculations reproduce hydro calculations for the SPS

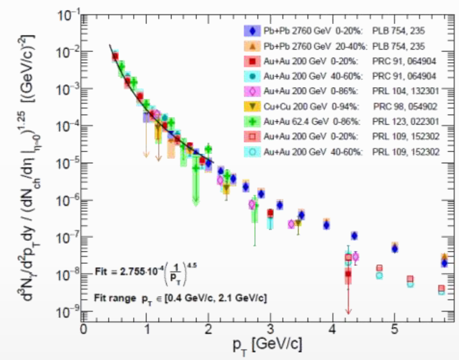

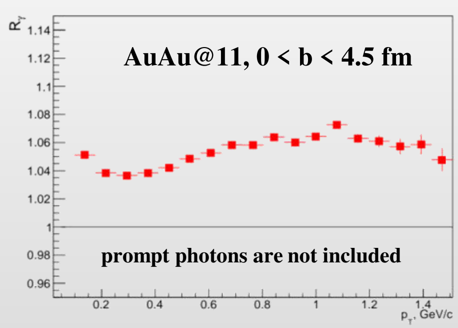

$$R_\gamma = \frac{\gamma_{inc}}{\gamma_{decay}} = \frac{\gamma_{inc}/\pi^0}{\gamma_{decay}/\pi^0_{param}}$$

$$\gamma_{direct} = \left(1 - \frac{1}{R_\gamma}\right) \cdot \gamma_{inc}$$

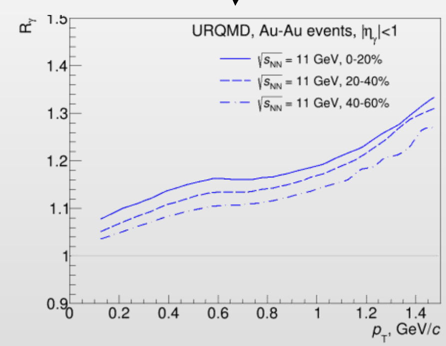

- Non-zero direct photon yields are predicted, Rγ ~ 1.05 – 1.15 → experimentally reachable by MPD!!!

Potentially, NICA can provide <u>unique measurements</u> for direct photons in the NICA energy range

Dielectron continuum and LVMs

- The QCD matter produced in A-A interactions is transparent for leptons, once produced they leave the interaction region largely unaffected + not sensitive to collective expansion
- Dielectron continuum at low and intermediate mass/p_T carries a wealth of information about reaction dynamics and medium properties:
  - ✓ low-mass part sensitive to late (hadronic) stage, intermediate mass — to hot stage
  - ✓ ρ-meson peak: modification of ρ-meson properties in hot matter (chiral phase transition)
  - ✓ charm production and correlations etc.

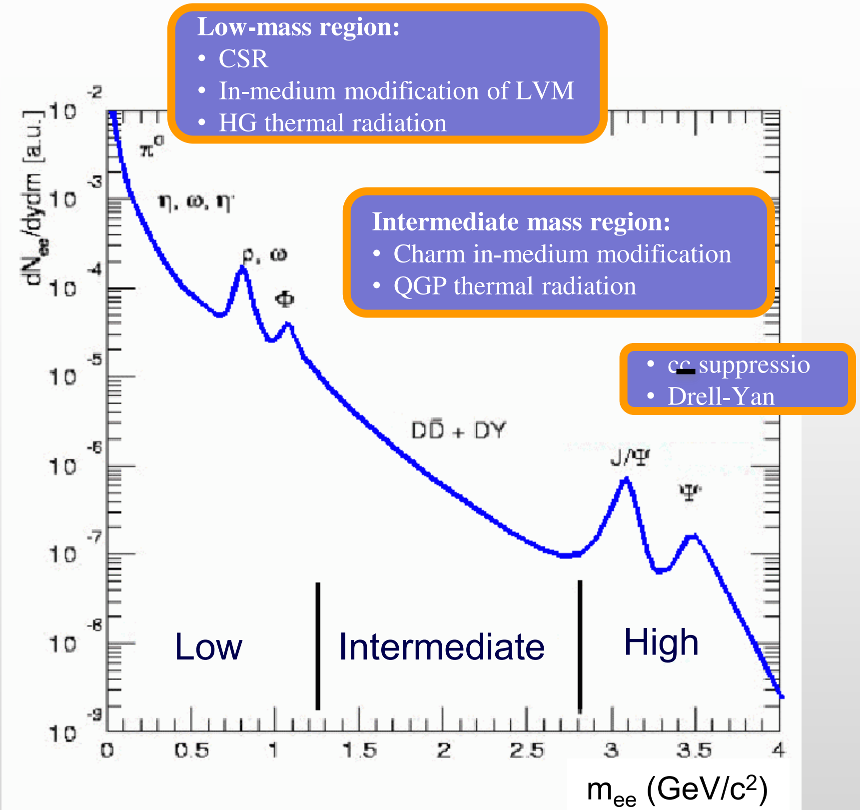

i	Dilepton channels	
1	Dalitz decay of π^0:	$\pi^0 \to \gamma e^+ e^-$
2	Dalitz decay of η:	$\eta \to \gamma l^+ l^-$
3	Dalitz decay of ω:	$\omega \to \pi^0 l^+ l^-$
4	Dalitz decay of Δ:	$\Delta \to N l^+ l^-$
5	Direct decay of ω:	$\omega \to l^+ l^-$
6	Direct decay of ρ:	$\rho \to l^+ l^-$
7	Direct decay of ϕ:	$\phi \to l^+ l^-$
8	Direct decay of J/Ψ:	$J/\Psi \to l^+ l^-$
9	Direct decay of Ψ':	$\Psi' \to l^+ l^-$
10	Dalitz decay of η':	$\eta' \to \gamma l^+ l^-$
11	pn bremsstrahlung:	$pn \to pn l^+ l^-$
12	$\pi^\pm N$ bremsstrahlung:	$\pi^\pm N \to \pi N l^+ l^-$

Experimental measurements

Last CERES result
PLB 666 (2008) 425

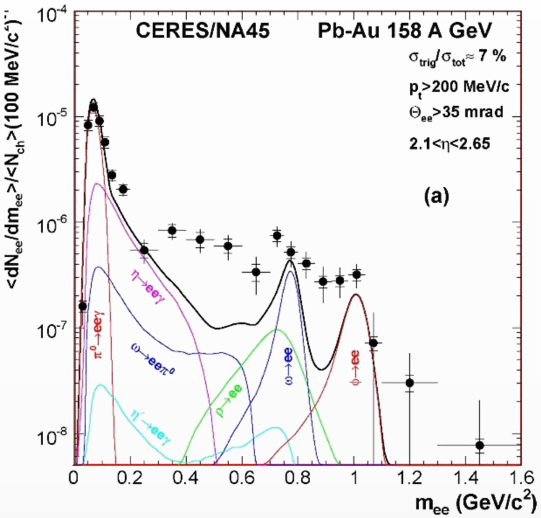

In+In 158 A GeV
PRL 96, 162302 (2006)

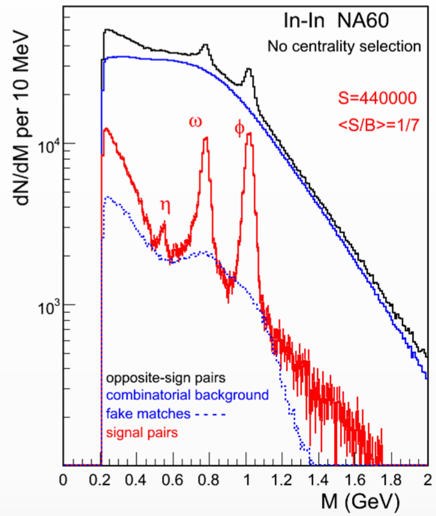

BES @ RHIC
PRL 113, 22301 (2014); PRC 92, 24912 (2015)

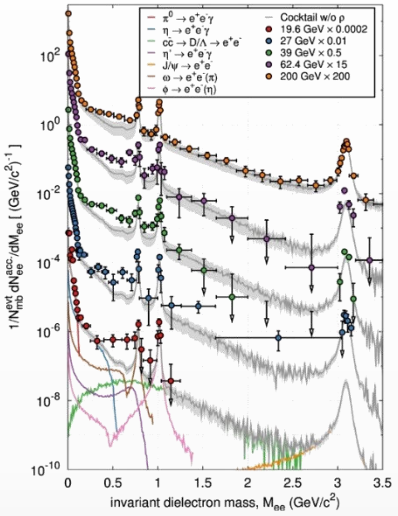

- ❖ A-A systems at all energies studied show:
  - ✓ LMR: clear enhancement of dileptons wrt to known hadronic sources → HG thermal radiation, broadening of ρ spectral shape
  - ✓ IMR: no clear picture, uncertainties for charm production
- ❖ Dilepton excess is consistently reproduced by microscopic many body model (Rapp et al.)

Prospects (I)

- Onset of deconfinement? Onset of CSR? Energy scan of dilepton excess:
  - Integrated yield in the LMR tracks the fireball lifetime
  - Inverse slope of the mass spectrum in the IMR provides a measurement of <T>, no blue shift
  - First order phase transition, "anomalous" variations in the fireball lifetime related to critical phenomena.?
  - Thermal radiation down to $\sqrt{s_{NN}}$ – 6 GeV ?

LMR as chronometer

PLB 753, 586 (2016)

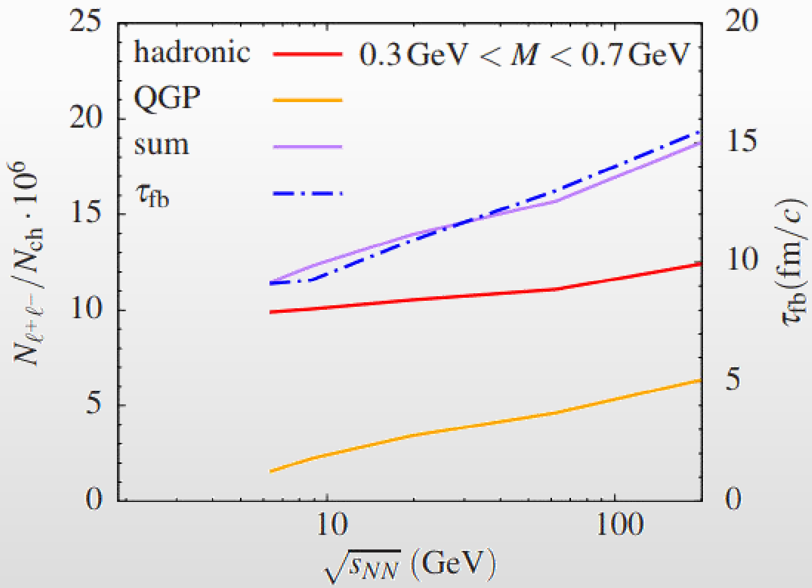

Integrated thermal excess radiation tracks the total fireball lifetime within ~ 10% → non-monotonous lifetime variations trace critical phenomena

IMR as thermometer

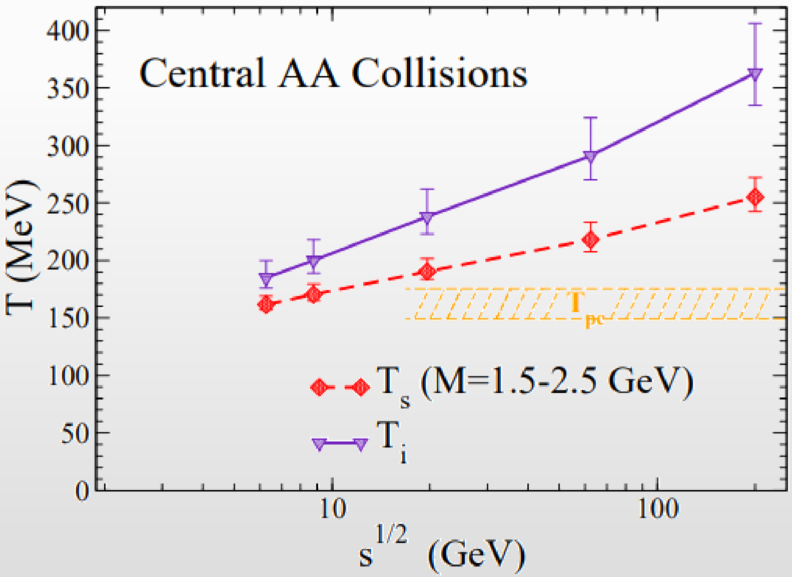

$dR_{ll}/dM \propto (MT)^{3/2} \exp(-M/T_s)$

T_s smoothly evolves T = 160 MeV to 260 MeV

Measured T_s is 15-30% below the initial T_i

Prospects (II)

- v_2 of thermal radiation
  - Very challenging measurement
  - v_2 as a function of p_T in different invariant mass regions probes the properties of the medium at different stages, from QGP to hadron-gas, provide an independent confirmation about the origin of the thermal radiation

Inclusive dielectron v_2
STAR PRC 90, 64904 (2014)

PHENIX, PRC 93, 014904 (2016)

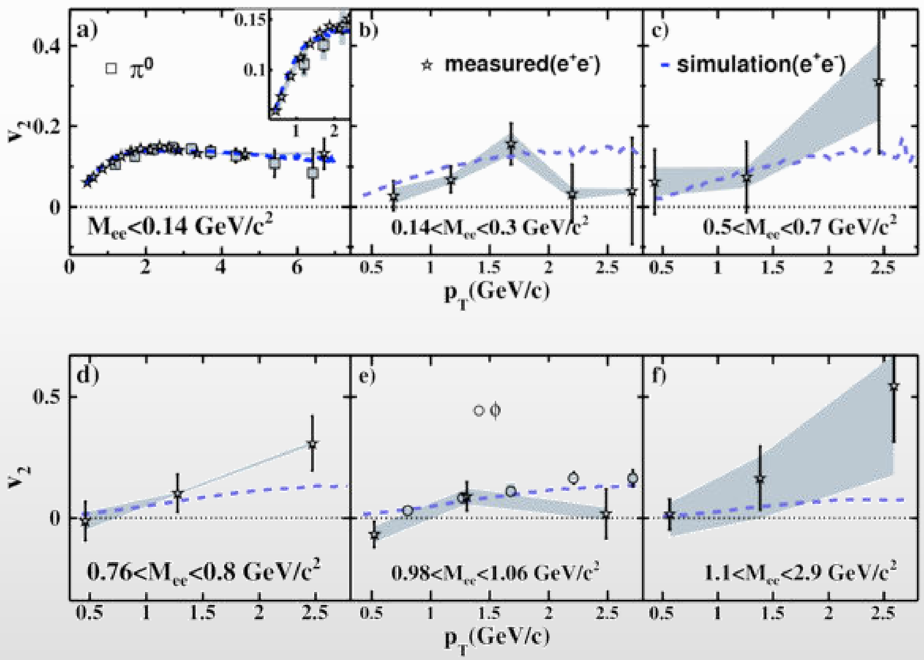

Challenge: isolate the v_2 of the excess dileptons

NICA → extensive program of dielectron measurements at $\sqrt{s_{NN}}$= 2-11 GeV

Conclusions

- ❖ Heavy-ion collisions provide the means to study QCD phase diagram at extreme temperatures and (net)baryon densities.
- ❖ A wide variety of different observables needs to be measured to characterize properties of the medium produced in heavy-ion collisions. Interpretation of experimental results requires close cooperation between experimentalists and theoreticians. Currently experiment drives development of HI physics
- ❖ Heavy-ion collisions are studied for over 30 years now, however, there is still a lot to be understood
- ❖ NICA is a megascience project in Russia, which is largely devoted to study of heavy-ion collisions → properties of QCD matter at moderate temperatures and maximum (net)baryon densities
- ❖ NICA is in final state of production, has capabilities for important/unique contributions

BACKUP

NICA Project

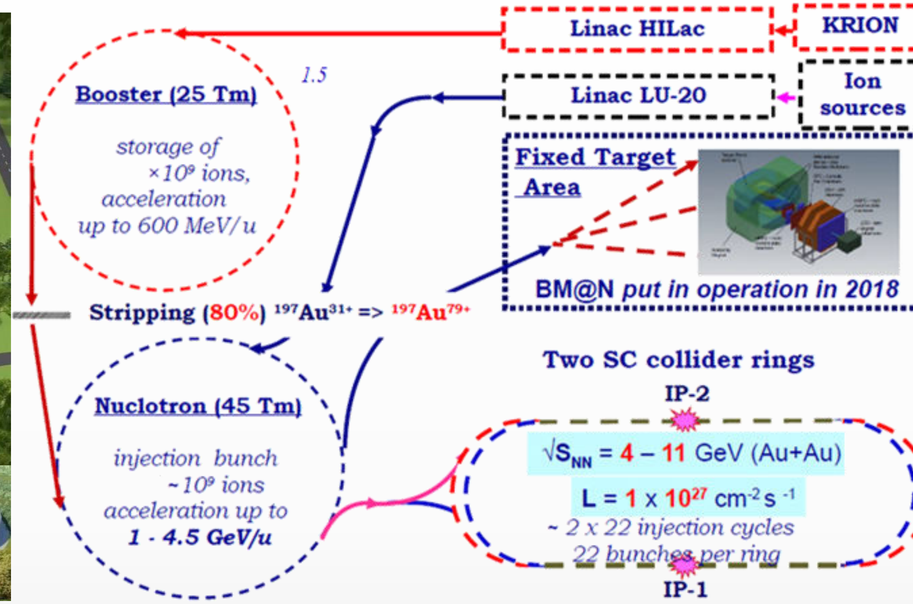

- The first megascience project in Russia, which is approaching its full commissioning:
  - ✓ already running in the fixed-target mode – BM@N
  - ✓ start of operation in collider mode in 2025 – MPD and later SPD
- Expected beam configuration in Stage-I:
  - ✓ Xe+Xe, Bi+Bi at $\sqrt{s_{NN}}$ = 4-11 GeV
  - ✓ heavy-ion beam luminosity up to ~10^{27} → collision rate ~ 5 kHz

STAR BES-I and BES-II Data Sets

Au+Au Collisions at RHIC

Collider Runs						Fixed-Target Runs					
	$\sqrt{s_{NN}}$ (GeV)	#Events	μ_B	y_{beam}	run		$\sqrt{s_{NN}}$ (GeV)	#Events	μ_B	y_{beam}	run
1	200	380 M	25 MeV	5.3	Run-10, 19	1	13.7 (100)	50 M	280 MeV	-2.69	Run-21
2	62.4	46 M	75 MeV		Run-10	2	11.5 (70)	50 M	320 MeV	-2.51	Run-21
3	54.4	1200 M	85 MeV		Run-17	3	9.2 (44.5)	50 M	370 MeV	-2.28	Run-21
4	39	86 M	112 MeV		Run-10	4	7.7 (31.2)	260 M	420 MeV	-2.1	Run-18, 19, 20
5	27	585 M	156 MeV	3.36	Run-11, 18	5	7.2 (26.5)	470 M	440 MeV	-2.02	Run-18, 20
6	19.6	595 M	206 MeV	3.1	Run-11, 19	6	6.2 (19.5)	120 M	490 MeV	1.87	Run-20
7	17.3	256 M	230 MeV		Run-21	7	5.2 (13.5)	100 M	540 MeV	-1.68	Run-20
8	14.6	340 M	262 MeV		Run-14, 19	8	4.5 (9.8)	110 M	590 MeV	-1.52	Run-20
9	11.5	157 M	316 MeV		Run-10, 20	9	3.9 (7.3)	120 M	633 MeV	-1.37	Run-20
10	9.2	160 M	372 MeV		Run-10, 20	10	3.5 (5.75)	120 M	670 MeV	-1.2	Run-20
11	7.7	104 M	420 MeV		Run-21	11	3.2 (4.59)	200 M	699 MeV	-1.13	Run-19
						12	3.0 (3.85)	2000 M	750 MeV	-1.05	Run-18, 21

Precision data to map the QCD phase diagram

3 < $\sqrt{s_{NN}}$ < 200 GeV; 750 < μ_B < 25 MeV

Angular momentum and magnetic field

System	Angular momentum (h/2π)
Electron in hydrogen atom	$\sqrt{l(l+1)}$
^{132}Ce (highest for nuclei)	70
Heavy-ion collisions	$10^4 - 10^5$

System	Vorticity (s^{-1})
Solar sub-surface	10^{-7}
Terrestrial atmosphere	10^{-5}
Great red spot of Jupiter	10^{-4}
Tornado core	10^{-1}
Heated soap bubbles	100
Turbulent flow in superfluid He	150
Heavy-ion collisions *STAR: Nature 548 (2017) 62*	$\mathbf{10^7 - 10^{21}}$

System	Magnetic Field in Tesla
Human brain	10^{-12}
Earth's magnetic field	10^{-5}
Refrigerator magnet	10^{-3}
Loudspeaker magnet	1
Strongest field in lab	10^3
Neutron star	10^6
Heavy-ion collisions	$\mathbf{10^{15} - 10^{16}}$

By orders of magnitude exceeds anything existing in the modern Universe

Polarization of Ξ and Ω

	Mass (GeV/c^2)	cτ (cm)	decay mode	decay parameter	magnetic moment (μ_N)	spin
Λ (uds)	1.115683	7.89	Λ->πp (63.9%)	0.732±0.014	−0.613	1/2
Ξ^- (dss)	1.32171	4.91	Ξ^-->Λπ^- (99.887%)	−0.401±0.010	−0.6507	1/2
Ω^- (sss)	1.67245	2.46	Ω^-->ΛK^- (67.8%)	0.0157±0.002	-2.02	3/2

- Λ, Ξ and Ω have different spins and magnetic moments, different number of s-quarks, less feedback for heavier hyperons
- Direct measurements are difficult due to small values of α
- Measured based on polarization of daughter Λ

Phys. Rev. Lett. 126, 162301 (2021)

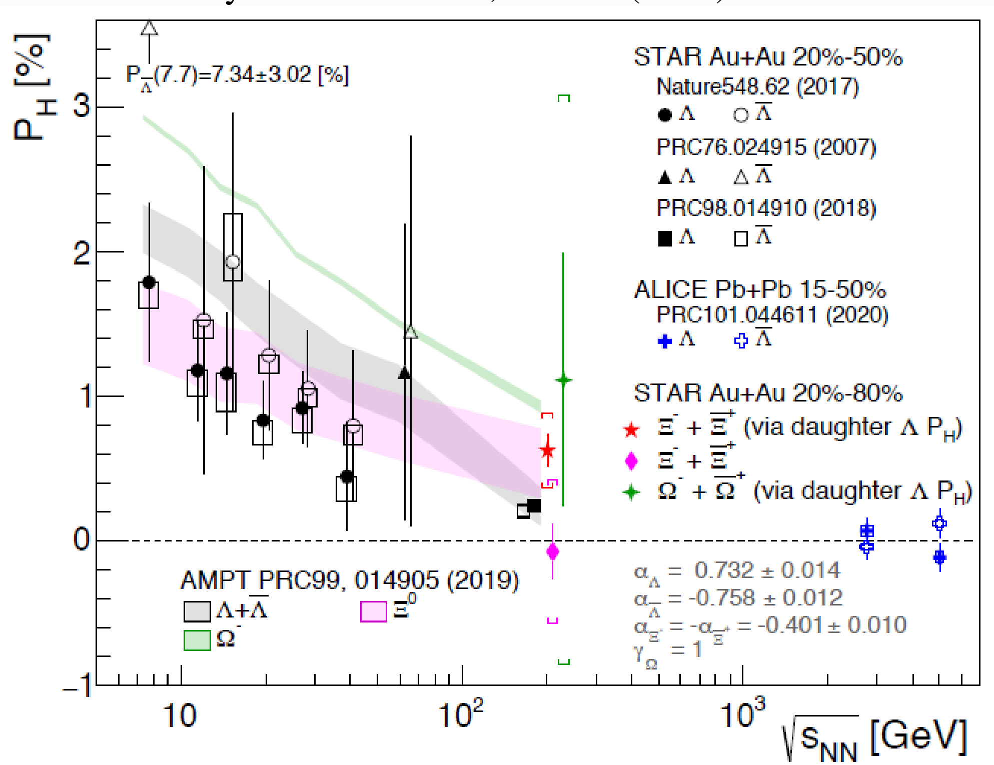

- AMPT is consistent with measurements
- Polarization of Ξ is larger compared with Λ:

$$\langle P_{\Lambda+\bar{\Lambda}}\rangle(\%) = 0.24 \pm 0.03 \pm 0.03$$

$$\langle P_{\Xi}\rangle = 0.47 \pm 0.10\ (\text{stat.}) \pm 0.23\ (\text{syst.})\ \%$$

- Λ results are not feed-back corrected (~ 15%)
- The AMPT is consistent with measurements
- Polarization of Ξ is larger compared with Λ
- Earlier freeze-out of multi-strange baryons is consistent with larger value of P_H for Ξ
- Large uncertainties for Ω, can expect larger signal, $P = \frac{\langle \bar{s}\rangle}{s} \sim \frac{s+1}{3}\frac{\bar{\omega}}{T}$ PRC95.054902 (2017)

Feed-down effect

- ~60% of measured Λ are feed-down from $\Sigma^* \to \Lambda\pi$, $\Sigma^0 \to \Lambda\gamma$, $\Xi \to \Lambda\pi$
- Polarization of parent particle R is transferred to its daughter Λ (Polarization transfer could be negative!)

$$\mathbf{S}^*_\Lambda = C\mathbf{S}^*_R \qquad \langle S_y \rangle \propto \frac{S(S+1)}{3}(\omega + \frac{\mu}{S}B)$$

$C_{\Lambda R}$: coefficient of spin transfer from parent R to Λ
S_R : parent particle's spin
$f_{\Lambda R}$: fraction of Λ originating from parent R
μ_R : magnetic moment of particle R

$$\begin{pmatrix} \varpi_c \\ B_c/T \end{pmatrix} = \begin{bmatrix} \frac{2}{3}\sum\limits_R \left(f_{\Lambda R}C_{\Lambda R} - \frac{1}{3}f_{\Sigma^0 R}C_{\Sigma^0 R}\right) S_R(S_R+1) & \frac{2}{3}\sum\limits_R \left(f_{\Lambda R}C_{\Lambda R} - \frac{1}{3}f_{\Sigma^0 R}C_{\Sigma^0 R}\right)(S_R+1)\mu_R \\ \frac{2}{3}\sum\limits_{\overline{R}} \left(f_{\overline{\Lambda R}}C_{\overline{\Lambda R}} - \frac{1}{3}f_{\overline{\Sigma^0}\overline{R}}C_{\overline{\Sigma^0}\overline{R}}\right) S_{\overline{R}}(S_{\overline{R}}+1) & \frac{2}{3}\sum\limits_{\overline{R}} \left(f_{\overline{\Lambda R}}C_{\overline{\Lambda R}} - \frac{1}{3}f_{\overline{\Sigma^0}\overline{R}}C_{\overline{\Sigma^0}\overline{R}}\right)(S_{\overline{R}}+1)\mu_{\overline{R}} \end{bmatrix}^{-1} \begin{pmatrix} P^{\rm meas}_\Lambda \\ P^{\rm meas}_{\bar{\Lambda}} \end{pmatrix}$$

Becattini, Karpenko, Lisa, Upsal, and Voloshin, PRC95.054902 (2017)

Decay	C
Parity conserving: $1/2^+ \to 1/2^+\ 0^-$	$-1/3$
Parity conserving: $1/2^- \to 1/2^+\ 0^-$	1
Parity conserving: $3/2^+ \to 1/2^+\ 0^-$	$1/3$
Parity-conserving: $3/2^- \to 1/2^+\ 0^-$	$-1/5$
$\Xi^0 \to \Lambda + \pi^0$	$+0.900$
$\Xi^- \to \Lambda + \pi^-$	$+0.927$
$\Sigma^0 \to \Lambda + \gamma$	$-1/3$

Primary Λ polarization will be diluted by 15%-20% (model-dependent)
This also suggests that **the polarization of daughter particles can be used to measure their parent polarization!** e.g. Ξ, Ω

Ξ and Ω polarization measurements

$$\frac{dN}{d\Omega^*} = \frac{1}{4\pi}(1 + \alpha_H \mathbf{P}_H^* \cdot \hat{\boldsymbol{p}}_B^*)$$

Getting difficult due to smaller decay parameter for Ξ and Ω…

$$\alpha_\Lambda = 0.732,\ \alpha_{\Xi^-} = -0.401,\ \alpha_{\Omega^-} = 0.0157$$

spin 1/2

Polarization of daughter Λ in a weak decay of Ξ:
(based on Lee-Yang formula)

T.D. Lee and C.N. Yang, Phys. Rev.108.1645 (1957)

$$\mathbf{P}_\Lambda^* = \frac{(\alpha_\Xi + \mathbf{P}_\Xi^* \cdot \hat{p}_\Lambda^*)\hat{p}_\Lambda^* + \beta_\Xi \mathbf{P}_\Xi^* \times \hat{p}_\Lambda^* + \gamma_\Xi \hat{p}_\Lambda^* \times (\mathbf{P}_\Xi^* \times \hat{p}_\Lambda^*)}{1 + \alpha_\Xi \mathbf{P}_\Xi^* \cdot \hat{p}_\Lambda^*}$$

$$\alpha^2 + \beta^2 + \gamma^2 = 1$$

$$\mathbf{P}_\Lambda^* = C_{\Xi^-\Lambda}\mathbf{P}_\Xi^* = \tfrac{1}{3}(1 + 2\gamma_\Xi)\mathbf{P}_\Xi^*.$$

$$C_{\Xi^-\Lambda} = +0.944$$

spin 3/2

Similarly, daughter Λ polarization from Ω:

$$\mathbf{P}_\Lambda^* = C_{\Omega^-\Lambda}\mathbf{P}_\Omega^* = \tfrac{1}{5}(1 + 4\gamma_\Omega)\mathbf{P}_\Omega^*.$$

Here **γ_Ω is unknown**.

- Time-reversal violation parameter β_Ω would be small
- α_Ω is very small

then $\gamma_\Omega \sim \pm 1$ and the polarization transfer $C_{\Omega\Lambda}$ leads to:

$$C_{\Omega\Lambda} \approx +1 \text{ or } -0.6$$

Parent particle polarization can be studied by measuring daughter particle polarization!

Polarization of vector mesons: $K^*(892)$ and ϕ

Non-central heavy-ion collisions:

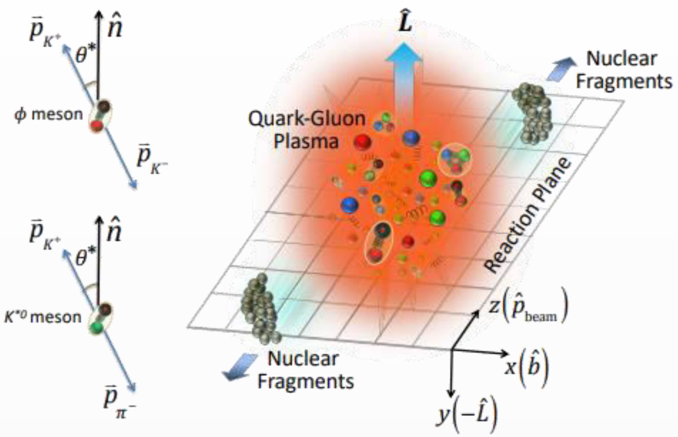

$$\frac{dN}{dcos\theta} = N_0\left[1 - \rho_{0,0} + cos^2\theta\left(3\rho_{0,0} - 1\right)\right]$$

$\rho_{0,0}$ is a probability for vector meson to be in spin state = 0 → $\rho_{0,0}$ = 1/3 corresponds to no spin alignment

The large ρ_{00} puzzle

$$\rho_{00} \approx \frac{1}{3} + C_\Lambda + C_\varepsilon + C_E + C_F + C_L + C_A + C_\varphi + C_g$$

Physics Mechanisms	(ρ_{00})
c_Λ: Quark coalescence vorticity & magnetic field[1]	< 1/3 (Negative ~ 10^{-5})
c_ε: E-comp. of Vorticity tensor[1]	< 1/3 (Negative ~ 10^{-4})
c_E: Electric field[2]	> 1/3 (Positive ~ 10^{-5})
c_F: Fragmentation[3]	> or, < 1/3 (~ 10^{-5})
c_L: Local spin alignments[4]	< 1/3
c_A: Turbulent color field[5]	< 1/3
c_φ: Vector meson strong force field[6]	> 1/3 (Can accommodate large positive signal)
c_g: Glasma fields + effective potential	could be significant

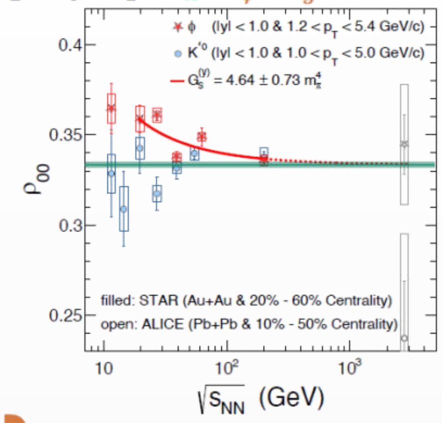

STAR, Nature 614 244 (2023)

strong force

Nature 614 244 (2023)

ϕ exhibits surprisingly large global spin alignment while K* displays little.

Aihong Tang. QuarkMatter 2023, Houston, Sept 3-9 18

- Measurements at RHIC/LHC challenge theoretical understanding → ρ_{00} can depend on multiple physics mechanisms (vorticity, magnetic field, hadronization scenarios, lifetimes and masses of the particles …)
- Measurements should be extended to lower collision energies

Critical fluctuations

- Ratio of the 4^{th}-to2^{nd} moment of the (net)proton multiplicity distribution:
  - ✓ non-monotonic behavior → deviation from non-critical dynamic baseline close to CEP ???

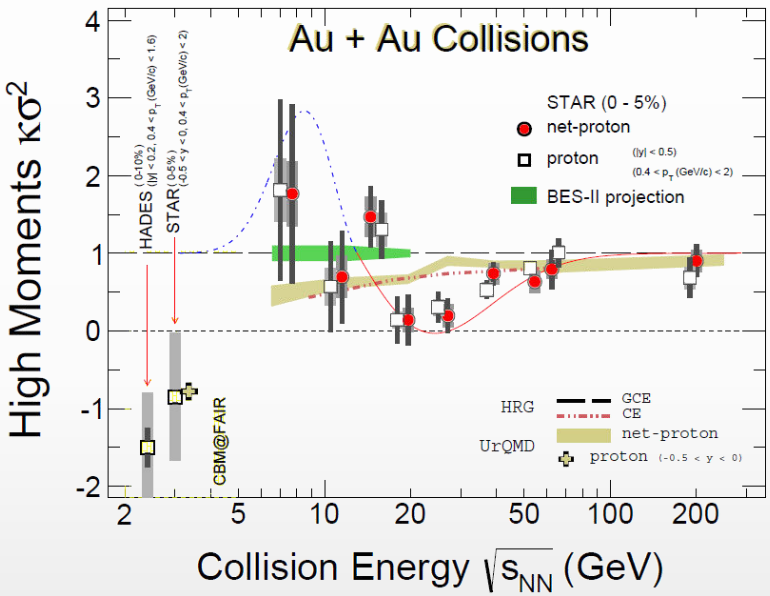

- Interpretation of results requires understanding of the role of finite-size effects, which have specific dependence on the size and duration of formed system

Significant <u>improvement of statistical precision and systematic</u> uncertainties and <u>extra points</u> in the NICA energy range are required

Hypermatter: intro

- Nuclear matter EOS is of importance for QCD, nuclear physics and astrophysics
- Only NN potential are very well determined from scattering experiments
- Hyperons appear in the core of neutron stars (NS) at approx. twice the normal nuclear density
- In a new chemical composition, due to attractive YN potentials, the EOS becomes softer
- New balance among the (inward) gravitational force and (outward) thermal + Fermi degenerate pressure impacts the mass-radius (M-R) relation for NSs

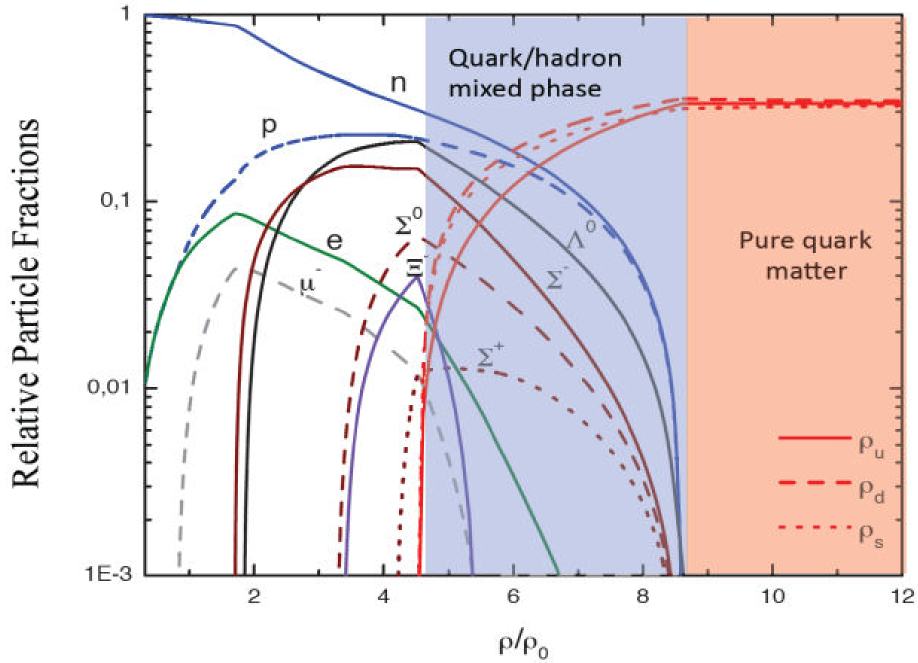

M. Orsaria et al, Phys. Rev. C 89, 015806 (2014)

Hypermatter in stellar objects: hyperon puzzle

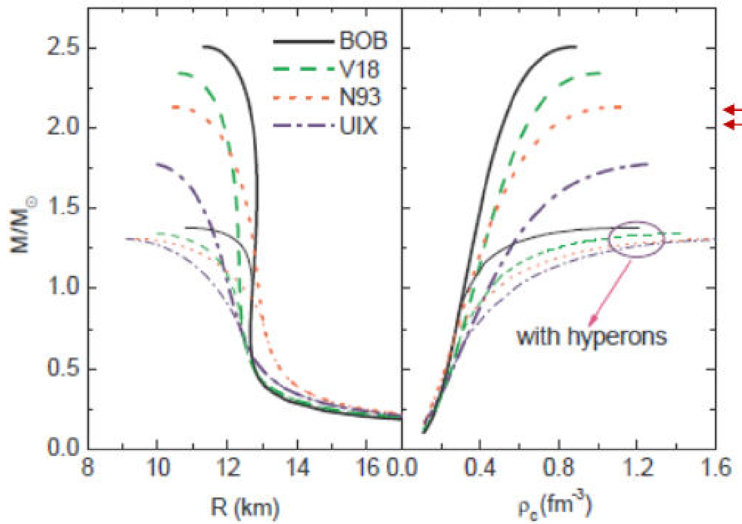

EoS becomes soft with hyperons → change in the M-R relation

2.17+/-0.11 (PSR J0740+662)
2.01±0.04 (PSR J0348+0432)

Contradiction with recent measurements for Millisecond Pulsar (MSP) masses

Hyperon Puzzle in NSs!

Proper description of the underlying hyperon-nucleon (YN) and hyperon-hyperon (YY) interactions in dense QCD medium is needed → hypernuclei offer the possibility.

High-energy heavy-ion reaction data

- Galactic Cosmic Rays composed of nuclei (protons, … up to Fe) and E/A up to 50 GeV
- These high-energy particles create cascades of hundreds of secondary, etc. particles

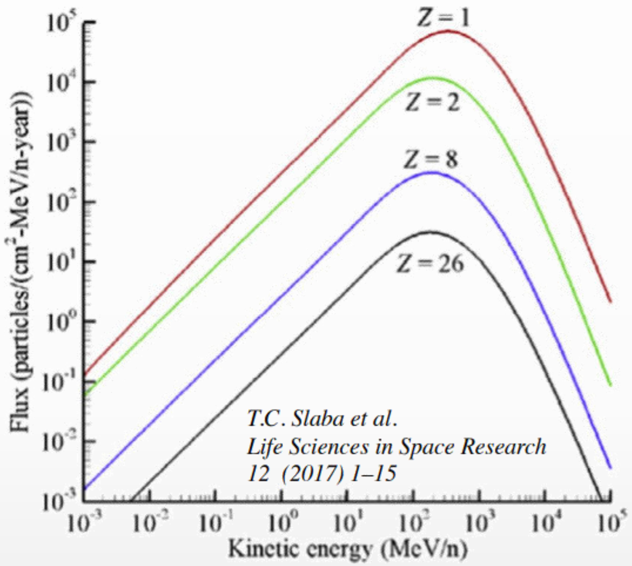

- Cosmic rays are a serious concern to astronauts, electronics, and spacecraft.
- The damage is proportional to Z^2, contribution of secondaries p, d, t, ^{3}He, and ^{4}He is also significant
- Need input information for transport codes for shielding applications (Geant-4, Fluka, PHITS, etc.):
  - ✓ total, elastic/reaction cross section
  - ✓ particle multiplicities and coellecense parameters
  - ✓ outgoing particle distributions: $d^2N/dEd\Omega$

High energy heavy ion reaction data

- NICA can deliver different ion beam species and energies:
  - ✓ Targets of interest (C = astronaut, Si = electronics, Al = spacecraft) + He, C, O, Si, Fe, etc.
- No data exist for projectile energies > 3 GeV/n

dE/dx vs momentum in TPC

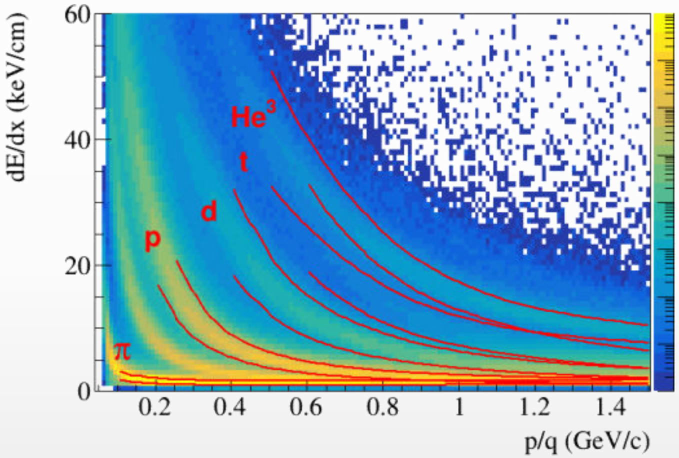

m^2 vs. momentum in TOF

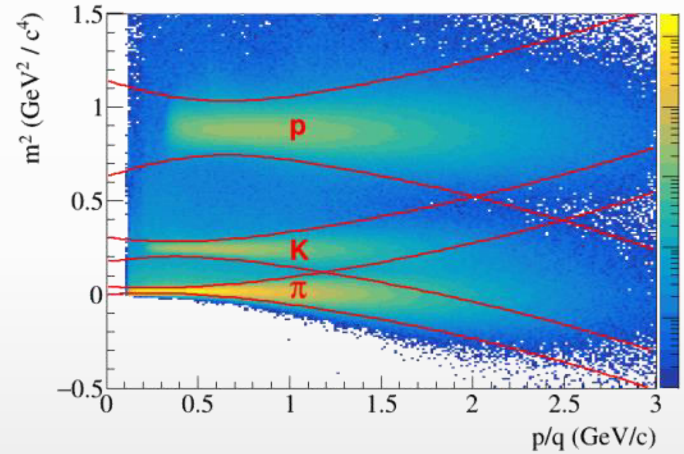

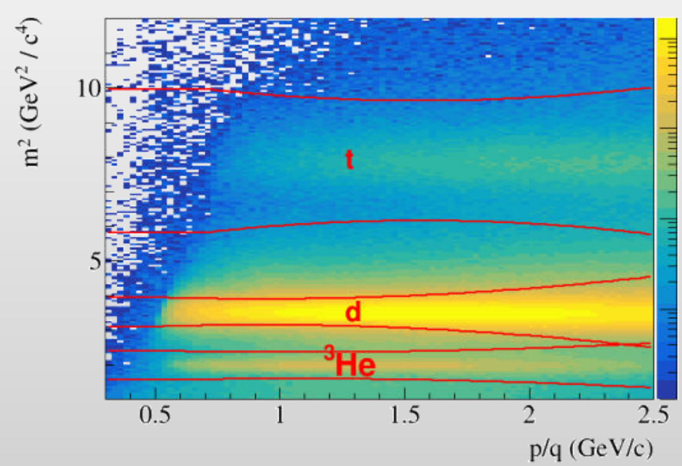

MPD has excellent light fragment identification capabilities in a wide rapidity range → unique capability of the MPD in the NICA energy range

Comparison to higher energies

- Rγ ~ 1.05-1.2 in heavy-ion collisions at SPS/RHIC/LHC, $\sqrt{s_{NN}}$ = 17.2-2760 GeV

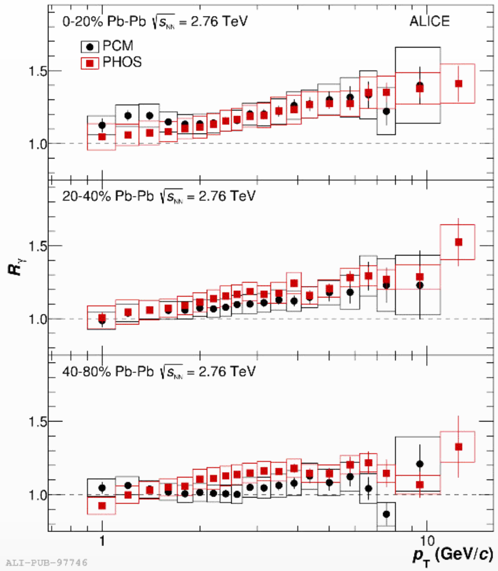

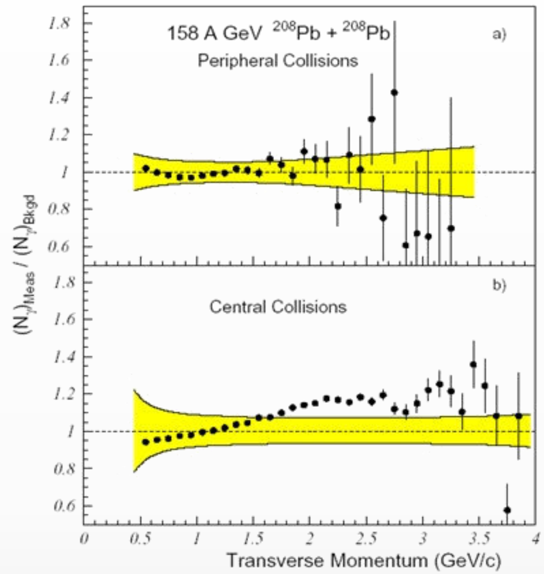

- Rγ ~ 1.05 is on the verge of experimental measurability (PHENIX in pp/pA@200, ≥ 2σ)

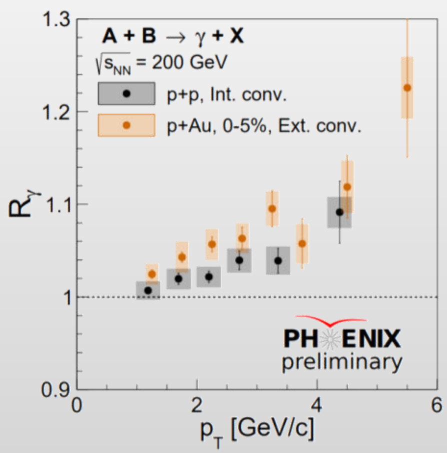

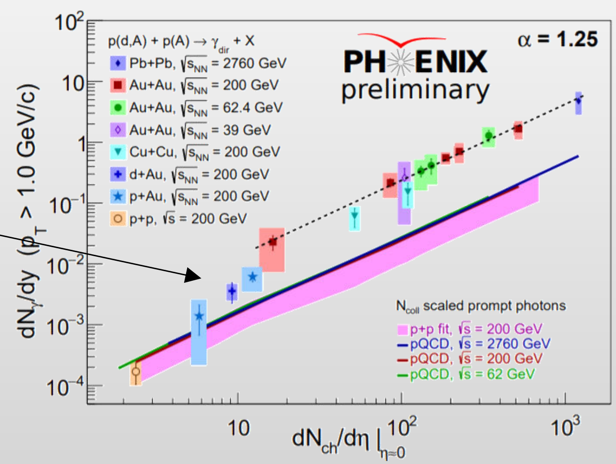

Dilepton experiments

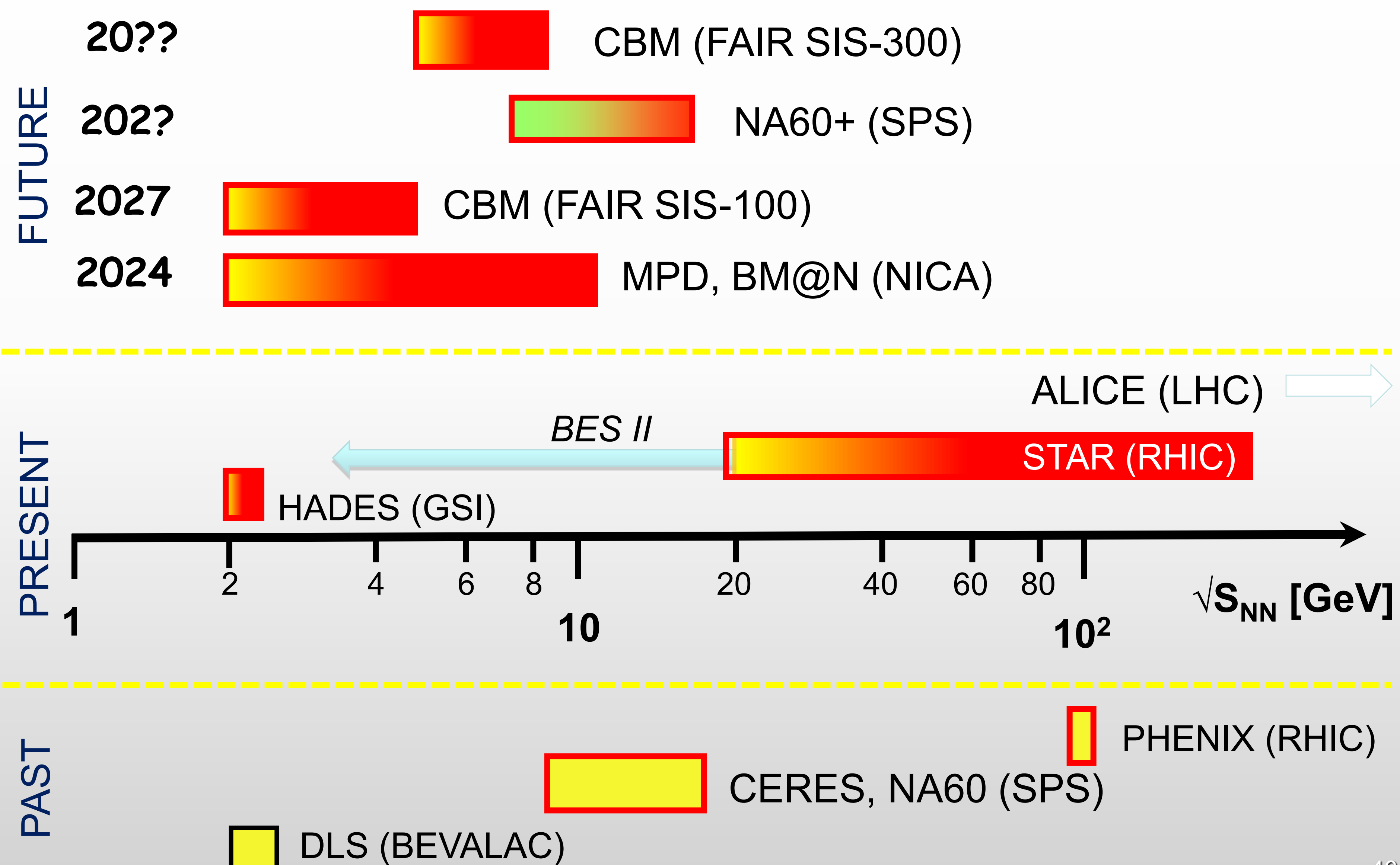

Electron identification

- Electrons are produced at low rates, $e/\pi \sim 10^{-3}$-10^{-4}
- Identification of electrons requires special treatment using capabilities of different detectors

TPC: log(dE/dx)

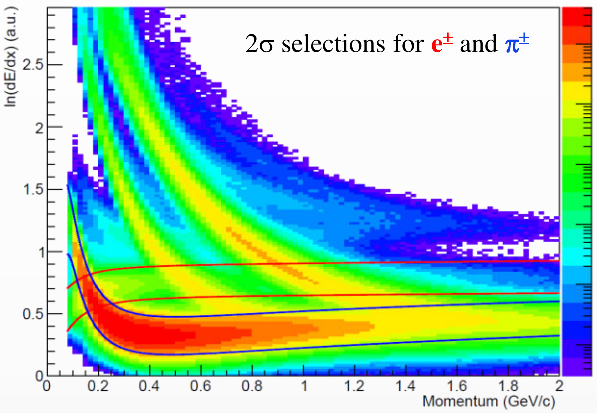

- ✓ eID at low momentum
- ✓ $e^{\pm}$ and $\pi^{\pm}$ bands merge at ~ 200 MeV/c

TOF: $\beta \sim 1$, $p_T > 150$ MeV/c

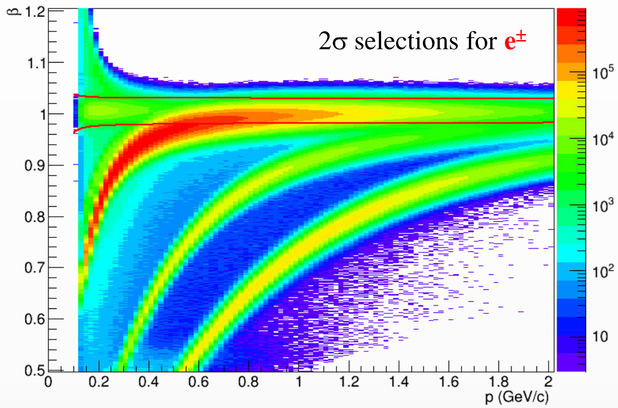

- ✓ $e^{\pm}$ with $p_T < 150$ MeV/c miss the TOF
- ✓ $e^{\pm}$ and $\pi^{\pm}$ bands merge at ~ 400 MeV/c

ECAL: tof < 2 ns ($\delta \sim 500$ ps) + $E/p \sim 1$

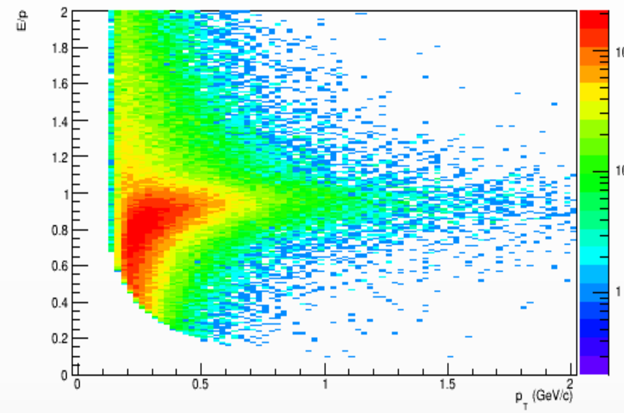

- ✓ $e^{\pm}$ with $p_T < 200$ MeV/c miss the ECAL
- ✓ $E/p \sim 1$ for $e^{\pm}$ at $p_T > 300$-400 MeV/c

- Each of the detectors provides more efficient electron identification in a limited range of momenta
- Combined use of the TPC-TOF-ECAL signals enhances the probability for a selected track to be true $e^{\pm}$

Electron efficiency and purity

- ❖ Simulated BiBi@9.2 GeV, realistic vertex distribution
- ❖ Selected tracks:
  - ✓ hits > 39
  - ✓ $|\eta| < 1$
  - ✓ |DCA_x,y,z| < 3 σ
  - ✓ 2σ matching to TOF
  - ✓ 1-2σ TPC-eID
  - ✓ 2σ TOF-eID

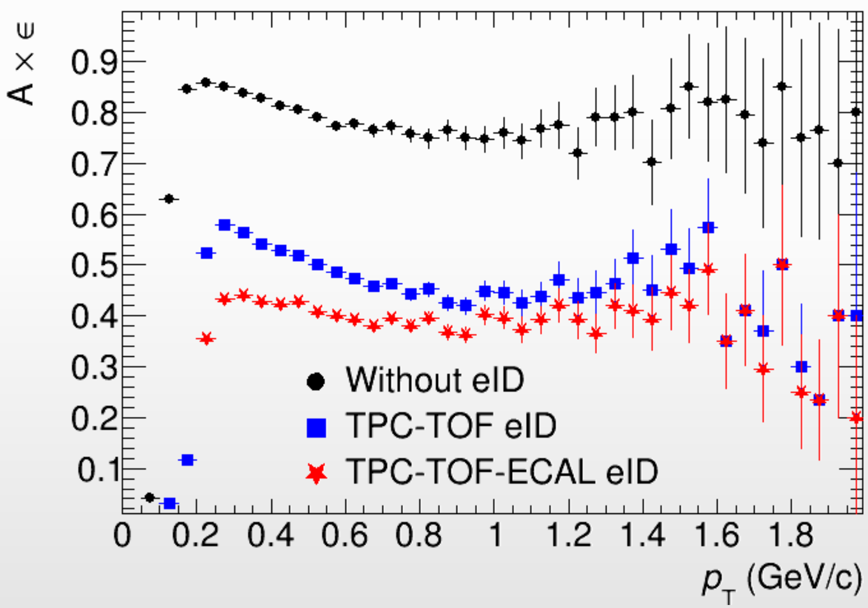

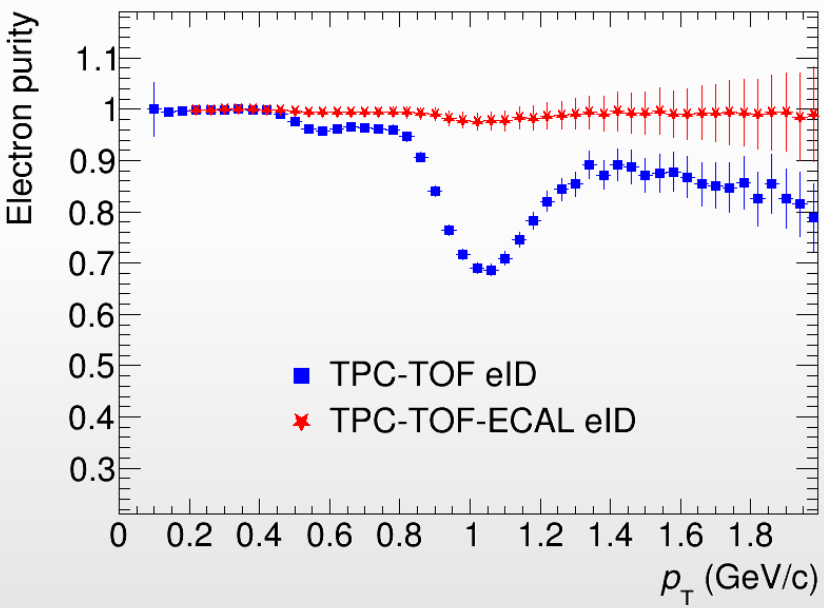

- ❖ Purity of ~ 100% at 40% reconstruction efficiency can be achieved at p_T > 150 MeV/c

JPS Conf. 32 (2020) 010079

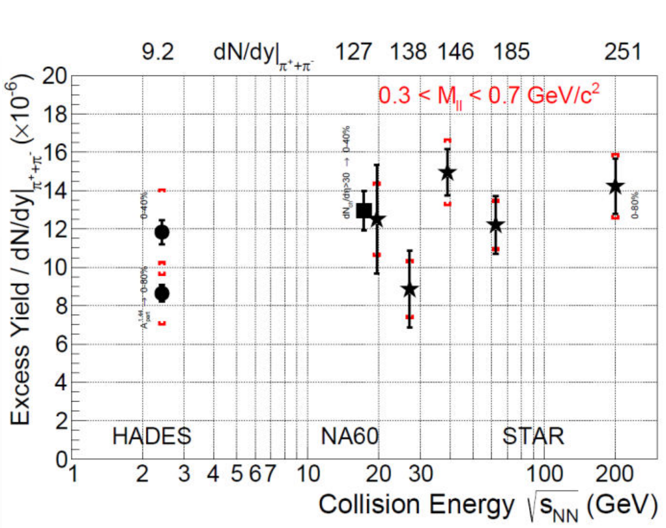

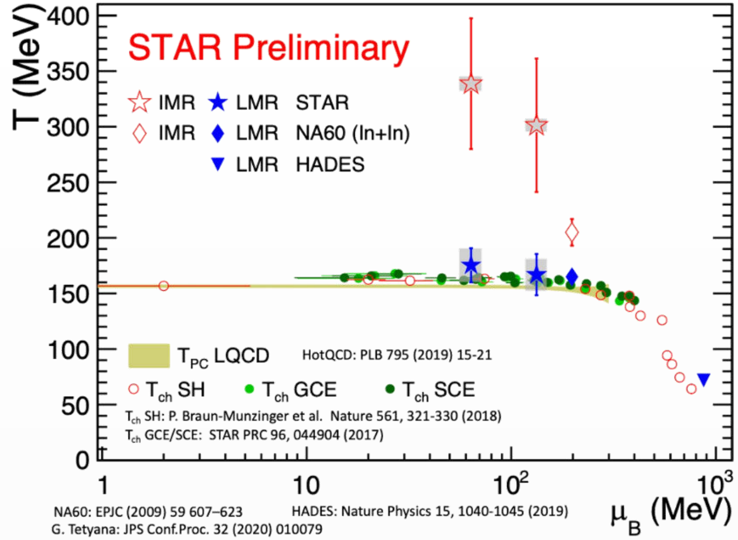

LMR as chronometer

PLB 753, 586 (2016)

IMR as thermometer

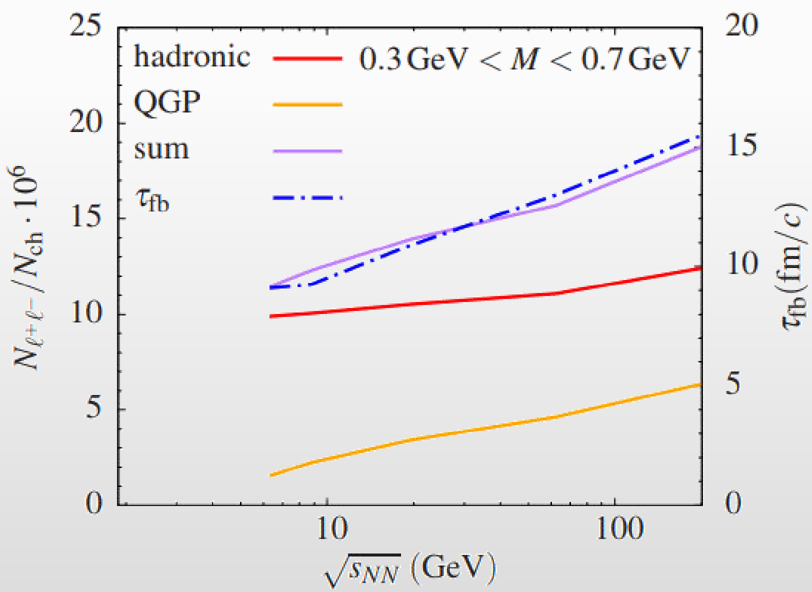

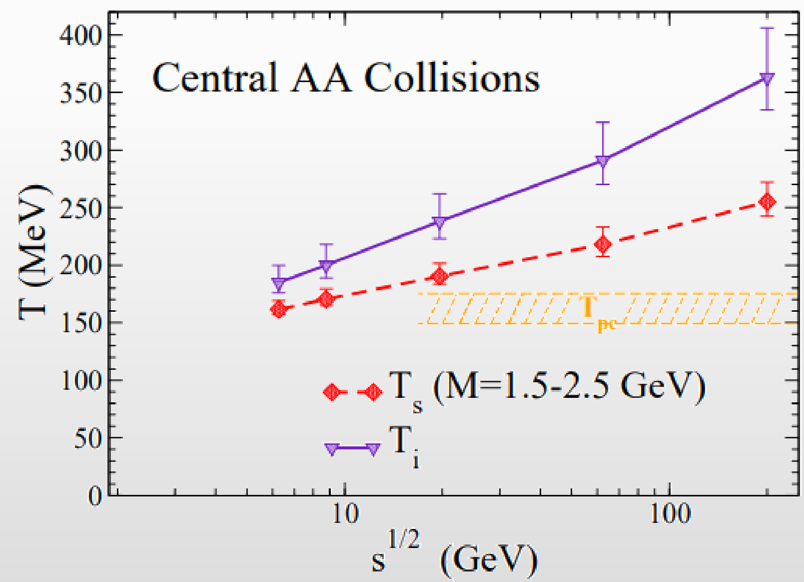

Integrated thermal excess radiation
tracks the total fireball lifetime within ~ 10% →
non-monotonous lifetime variations trace critical phenomena

$dR_{ll}/dM \propto (MT)^{3/2} \exp(-M/T_s)$
T_s smoothly evolves T = 160 MeV to 260 MeV
Measured T_s is 15-30% below the initial T_i

- Yield and flow of e+e- pairs:
  - ✓ probe deconfinement and chiral symmetry restoration
  - ✓ effective temperature

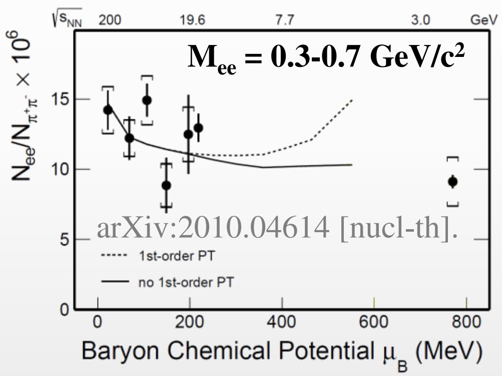

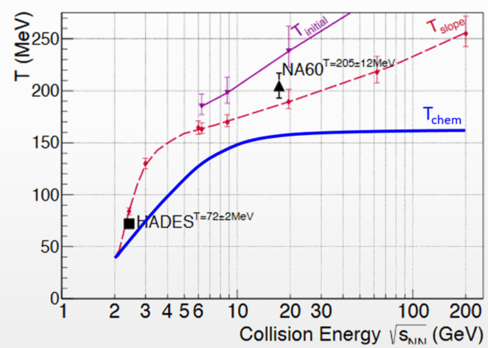

T. Galatyuk et al., Eur. Phys. J. A 52 (2016) 131; R. Rapp and H. v. Hess, PLB 753 (2016) 586
J.Cleymans et al. 2006 Phys. Rev. C73, 034905
NA60: H. Specht, AIP Conf. Proc. 1322 (2010) 160; HADES: Nature Physics 15 (2019) 1040